FINAL REPORT

U.S. Department of Energy

Rapid Migration of Radionuclides Leaked from High-Level Water Tanks: A Study of Salinity Gradients, Wetted Path Geometry and Water Vapor Transport

Principal Investigator: Anderson L. Ward
Pacific Northwest National Laboratory
P.O. Box 999, MSIN K9-33
Richland, WA 99352-9999
Email: andy.ward@pnl.gov

Co-Principal Investigator: Glendon W. Gee
Pacific Northwest National Laboratory
P.O. Box 999, MSIN K9-33
Richland, WA 99352
Email: glendon.gee@pnl.gov

Collaborator: John S. Selker
RM 240 Gilmore Hall
Oregon State University
Corvallis, OR 97331-3906
Email: selkerj@engr.orst.edu
Grant Number: DE-FG07-98ER14925

Collaborator: Clay Cooper
Division of Hydrologic Sciences
Desert Research Institute
2215 Raggio Parkway
Reno, NV 89512-1095
Email: clay@dri.edu
Grant Number: DE-FG07-98ER14920

Project Number: 65410
Project Duration: October 1, 1998 to September 30, 2001

Contents

Executive Summary

The basis of this study was the hypothesis that the physical and chemical properties of hypersaline tank waste could lead to wetting front instability and fingered flow following a tank leak. Thus, the goal of this project was to develop an understanding of the impacts of the properties of hypersaline fluids on transport through the unsaturated zone beneath Hanford's Tank Farms. There were three specific objectives (i) to develop an improved conceptualization of hypersaline fluid transport in laboratory (ii) to identify the degree to which field conditions mimic the flow processes observed in the laboratory and (iii) to provide a validation data set to establish the degree to which the conceptual models, embodied in a numerical simulator, could explain the observed field behavior. As hypothesized, high ionic strength solutions entering homogeneous pre-wetted porous media formed unstable wetting fronts atypical of low ionic strength infiltration. In the field, this mechanism could force flow in vertical flow paths, 5-15 cm in width, bypassing much of the media and leading to waste penetration to greater depths than would be predicted by current conceptual models. Preferential flow may lead to highly accelerated transport through large homogeneous units, and must be included in any conservative analysis of tank waste losses through coarse-textured units. However, numerical description of fingered flow using current techniques has been unreliable, thereby precluding tank-scale 3-D simulation of these processes. A new approach based on nonzero, hysteretic contact angles and fluid-dependent liquid entry has been developed for the continuum scale modeling of fingered flow. This approach has been coupled with and adaptive-grid finite-difference solver to permit the prediction of finger formation and persistence form sub centimeter scales to the filed scale using both scalar and vector processors. Although laboratory experiments demonstrated that elevated surface tension of imbibing solutions can enhance vertical fingered flow, this phenomenon was not observed in the field. Field tests of showed that the fingered flow behavior was overwhelmed by the variability in texture resulting from differences in the depositional environment. Field plumes were characterized by lateral spreading with an average width to depth aspect ratio of 4. For both vertical fingers and lateral flow, the high ionic strength contributed to the vapor phase dilution of the waste, which increased waste volume and pushed the wetting front well beyond what would have occurred if the volume of material had remained unchanged from that initially released into the system. It was also observed that following significant vapor-phase dilution of the waste simulants that streams of colloids were ejected from

the sediment surfaces. It was shown that due to the high-sodium content of the tank wastes the colloids were deflocculated below a critical salt concentration in Hanford sediments. The released colloids, which at the site would be expected to carry the bulk of the sorbed heavy metals and radioisotopes, were mobile though coarse Hanford sediments, but clogged finer layers. The developments resulting from this study are already being applied at Hanford in the nonisothermal prediction of the hypersaline, high pH waste migration in tank farms and in the development of inverse methods for history matching under DOE's Groundwater/Vadose Zone Integration Project at Hanford.

1.0 Research Objectives

Field observations at Hanford show reactive contaminants (e.g. cesium-137) normally assumed to be strongly adsorbed by soil to be nearly twice as deep as predicted by numerical models based on existing conceptualizations of vadose zone transport. The discrepancy between field observations and predictions raised concerns about the ability to describe and predict the distributions of waste fluids leaked from single-shelled tanks and about strategies for retrieving waste from these tanks. The retrieval method of choice, hydraulic sluicing, could potentially result in deep penetration of fluids leaked during the process and the remobilization of exiting plumes with possible impacts on groundwater.

The objectives of this study were:

(1) to develop an improved conceptualization of hypersaline fluid transport in laboratory

(2) to identify the degree to which field conditions mimic the flow processes observed in the laboratory and

(3) to provide a validation data set to establish the degree to which the conceptual models, embodied in a numerical simulator, could explain the observed field behavior.

Laboratory studies were conducted to establish the fundamentals of flow and transport under a range of fluxes of saline fluids using Miller similar sands. Studies at Oregon State University (OSU) focused on the investigation of the effect of wetting front instability and vapor flux on plume mobility. Work at The Desert Research Institute (DRI) focused on characterizing the hydraulic properties of Hanford sediments and the dependence of these properties on fluid composition. Studies at the Pacific Northwest National Laboratory (PNNL) studied the behavior of these fluids in native Hanford sediments and the development of a conceptual and numerical model to predict field-scale behavior.

2.0 Methods

Addressing the goals of this proposal required significant advances in our conceptualization of the transport mechanisms and novel laboratory experiments to determine the degree to which these effects would be manifested under field conditions. The research plan, therefore, included significant components of controlled laboratory experiments, numerical simulation, and field trials. The methods used in each component are discussed separately below.

2.1 Controlled Laboratory Experiments

The controlled laboratory studies were aimed at understanding the fundamental mechanisms controlling the movement of hypersaline fluids in unsaturated sediments. Different aspects of the laboratory studies were conducted by each of the collaborating institutions and included infiltration studies in commercial quartz (Miller similar) sands; characterization of the hydraulic properties of Hanford sediments and the dependence of these properties on fluid composition; and infiltration tests in Hanford sediments.

2.1.1 Infiltration of Hypersaline Fluids in Miller Similar Sands

A light transmission system was used to quantify liquid content in two-dimensional (2D) flow cells in space and time. The light transmission system consisted of three primary components: chamber, light source, and detector (Figure 1a). The media-containing portion of the light transmission system, referred to as the chamber, consisted of two, 1.27-cm-thick × 50.0-cm-wide × 65.0-cm-high, glass panels separated by a 1.0-cm-thick U-shaped aluminum spacer. The glass sheets were sealed to the spacer by 4.8-mm diameter rubber O-ring stock contained within continuous channels machined on both faces of the spacer. A drain-port through the bottom of the spacer allowed exchange of fluid within the system. A 1.0-cm-thick acrylic manifold topped with 200-mesh stainless steel wire screen provided the lower media boundary. The chamber components were compressed together within a rubber-lined aluminum frame. The resulting inner chamber thickness was 1.0 cm (Figure 1b). All aluminum parts were anodized black to avoid reflections. A detailed description of the flow cell, visualization apparatus, and data interpretation methods are presented by Wesibrod et al(2002) and Niemet et al (2001).

All infiltration tests were conducted in Accusand® (Unimin, Le Sueur, MN), a well-defined, homogenous, translucent silica sands with the 12/20, 20/30, 30/40, and 40/50 grades. A detailed description of the Accusand® properties are reported in *Schroth et al*. [1996]. Prior to the infiltration tests, the sand was rinsed multiple times with deionized until there was no turbidity in the supernatant. The sand was then dried for 48 hrs at 45°C. Five different solutions were used for the infiltration experiments, water, sodium nitrate, and sodium nitrate + methanol (Table 1). The addition of nitrate to the solutions raised the surface tension and viscosity by promoting hydrogen bonding strength to create a tank waste simulant. The addition of 2 vol.% of methanol to the 5 molal sodium nitrate solution lowered the surface tension to the 72 mN m^{-1} of pure water while only slightly lowering viscosity and density.

Table 1. Physical Properties of Test Fluids.

Solution	Composition	Density g cm^{-3}	Viscosity cp	Surface tension mN m^{-1}
A	5 molal $NaNO_3$	1.247	1.314	80.54
B	5 molal $NaNO_3$ + 2% methanol	1.199	1.034	70.28
C	Pure water	0.993	1.001	72.8
D	2 molal $NaNO_3$	1.095	1.117	75.19
E	0.75 molal $NaNO_3$	1.037	1.036	73.69

Experiments were conducted in 12/20, 20/30, 30/40, and 40/50 grades of Accusands. In all experiments, the chamber was prepared and packed with a single sand grade as described in *Niemet and Selker* [2001]. The pore space was purged with at least 10 pore volumes of CO_2 gas, slowly delivered through the lower port. Next, distilled water, solution ***C,*** was delivered through the same port at ~ 20 mL/min until the media was saturated, with the exception of Exp. 7, in which solution ***A*** was used for the wetting process. To ensure complete saturation and removal of dissolved CO_2, four additional pore volumes of water were passed through the sand. The porosity of each pack was determined based on the volume of fluid required to saturate the sand, the mass of sand, and the overall internal volume of the chamber. Images were taken prior to

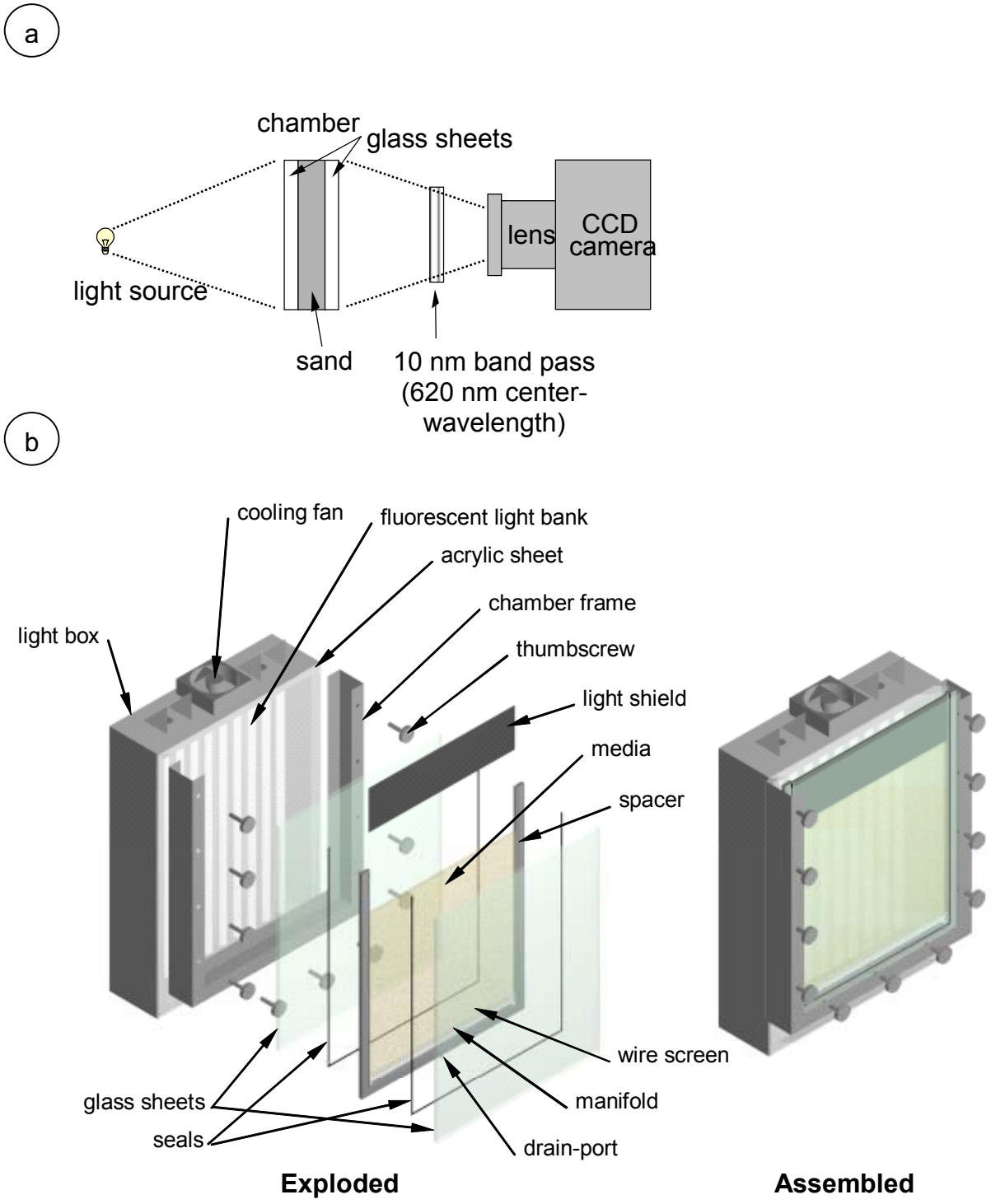

Figure 1. (a) Major optical components of the light transmission system and (b) exploded and assembled views of the light transmission chamber.

and following saturation in all experiments, which were termed the "dry" and "saturated" images, respectively. After saturation, the chamber was allowed to slowly drain (< 10 mL min^{-1}) for 24 hours, with the zero-pressure level held at the height of the manifold's upper surface.

Following drainage the outflow pipe was closed in all experiments, excluding Exp. 7. The vertical extent of saturated media (capillary fringe height) ranged from 7.5 to 23 cm above the manifold surface, depending upon sand grade.

Typically, three evenly spaced 5 mL solution applications (Table 1) were dripped at a rate of 1 mL min^{-1} onto the surface of the sand. An image was taken immediately after application, followed by imaging at 10 min intervals for the first 3 h after the injection, at 1 h intervals from 3-24 h after the injection, at 2 h intervals from 24-48 h after the injection, and at 3 h intervals from 48-72 h after the injection. In some of the experiments, additional images were taken after 72 h. The total number of images ranged from 48 to 78 per experiment.

Image processing and data analysis

Post-experiment image processing to determine water saturation from the raw data images was performed using the method of *Niemet and Selker* [2001]. After removing the bias and dark signals from the images, the relative degree of light transmission was computed on a pixel-by-pixel basis. The log-scaled relative degree of light transmission was then determined and the effective degree of saturation computed from a 4^{th}-order polynomial approximation, unique to each of the sands. The processed images provide a pixel-by-pixel spatial distribution of the changes in saturation. Changes in saturation from 0 to 32% are shown, with each band representing a 2% change. The gray scale proceeds from black (least change) to light gray (greatest change), with white reserved for the 0 to 2% interval. All image processing was performed using Transform 3.4 (Fortner Software LLC).

To better distinguish the wetting front contours, two smoothing passes were performed on the saturation change images. In each smoothing pass every pixel was averaged with its eight neighbors. Incremental wetting front velocities were calculated from the vertical distance traveled by the wetting front over the time between consecutive images. These velocities describe the dynamic behavior of the plumes as they evolve, and provide information about the flow process within a restricted depth interval for the conditions at that time.

2.1.2 Infiltration of Hypersaline Fluids in Hanford Sediments

The goal of these studies were to investigate the infiltration behavior of hypersaline fluids, particularly sodium nitrate, in sediments from the Hanford Formation. The mineralogy of these sediments is dominated by dark colored anorthitic plagioclase and ferromagnesian minerals, which render them immune to investigation by light visualization. Infiltration behavior was investigated at PNNL using X-Ray Microfocus Tomography (XMT) in 5 cm o.d. x 15 cm long acrylic columns. The XMT system is capable of achieving a resolution in the focal plane of one one-thousandth of the object diameter. A microfocus X-ray source allows variable slice widths over a nominal range of 10 to 150 μm and can also be used to obtain digital radiographs. The system is composed of a Kevex model KM16010E-A X-ray tube with spot sizes of 10, 20, 65, 250 μm at power levels 5, 10, 50, and 160 watts, respectively. A computer data acquisition, instrument control, and image reconstruction system with the ACTIS+ software provides X-ray and sample manipulation control in addition to CT and CT Multi-Planer (MPR-3D) image.

Experiments were conducted in undisturbed and repacked sediments from the site used for the field experiments (Section 2.2) and with homogeneous fractions silt, fine sand, and coarse sands. Control columns were packed with 20/30 and 30/40 grades of Accusand. The effect of antecedent moisture was investigated by comparing initially dry columns with columns pre-wetted with deionized water. Prior to the infiltration tests, the pore space was purged with at least 10 pore volumes of CO_2 gas, slowly delivered through the base of the column. A 3 mL pulse of sodium iodide was injected at a rate of 1 mL min^{-1} onto the surface of each column and subsequently imaged by the XMT at 10-min. intervals for the first 60 minutes and then after 24 hrs of redistribution. The shape and dimensions of the each sodium iodide plume were recorded and compared.

2.1.3 Contact Angle of Hypersaline Fluids on Silica Sands

The goal of this study was to determine if different contact angles develop for pure water and saline solution during infiltration into porous media. Specific objectives included: (1) a comparison of static and dynamic methods of contact angle measurement; (2) identify an appropriate model for predicting observed wetting front behavior, and (3) a comparison of the contact angles developed by pure water and hypersaline solution in air-dry and pre-wetted sands. Detailed discussions of the experimental methods and results are presented in McGinnis (2001) and McGinnis et al (2001). Briefly, in this study, both static and dynamic methods were used to estimate the contact angle formed by solutions of varying surface tension on Accusands. In addition, the contact angle of the imbibing solutions was estimated in both dry and sand pre-wetted with a salt-free solution. The rationale for using pre-wetted (but unsaturated) sand was to create a more realistic environment for the imbibing solutions being tested, as it is well known that most soils have a non zero residual moisture content.

Both static (Letey et al. 1962) and dynamic (Washburn, 1921) methods were used to determine contact angles. In the static method, the capillary pressure and the gravitational pressure are taken to be in equilibrium when the system is at steady state. By invoking the capillary bundle model for a porous medium, $\Delta P = 2\gamma \cos\phi r^{-1}$, an effective pore radius, r, is assumed. Measuring the height of capillary rise in a packed column of soil with a perfectly wetting fluid (zero contact angle) allows calculation of the pore radius, r. Imbibition of a second fluid of unknown contact angle into another pack, with the assumption that r remains unchanged, allows calculation of the contact angle, ϕ.

In this test, n-hexane was used as the perfectly wetting fluid because it wets quartz with an apparent contact angle 0° at room temperature. The dynamic method is based on the theory of (Washburn, 1921). The theory indicates that if a porous solid is brought into contact with a liquid (not submerged), then the imbibition of liquid into the pores of the solid due to capillary action (ignoring gravity) scales with the square root of time. Assuming the density, viscosity, and surface tension of the liquid are known, and measuring mass of liquid that rises into the sand over time allows calculation of the contact angle. As in the static method, n-hexane was used in order to determine the material constant for the porous media tested, which is assumed to remain unchanged between packings. Repeating the measurements on a second column with the fluid of interest allow calculation of the contact angle.

Experiments in this study employed three clear acrylic columns of known volume to determine contact angles using two methods, one static method and one dynamic method. The three acrylic columns were packed with the same mass of each grade of Accusand® (40/50, 30/40, 20/30, and 12/20 grades respectively) for triplicate measurements. The solutions used in this study included (1) pure water and (2) 5 molal sodium nitrate and (3) n-hexane as a reference.

2.1.4 Contact Angle of Hypersaline Fluids on Hanford Sediments

There is evidence of the existence of a dynamic contact angle that is generally larger than the static or equilibrium value, even for totally wetting liquids. However, the precise conditions determining dynamic contact angle behavior are not well understood. Determination of the contact angle allows characterization of the wetting behavior of the solid and quantification of effect of the fluid. The aim of this component of the study was to determine whether the nature of the infiltrating fluid had any affect on the dynamic contact angle in real soils. This study used a different approach to estimating the contact angle than that described in 2.1.3. The Washburn method is based on the premise that the two cores, one for measurement with a reference liquid, and one for the liquid of interest, are identical. Unlike the Accusands, sediments from the Hanford Formation are mineralogically heterogeneous and particle shape is typically nonuniform. For this type of material, the pore radius, *r*, of the capillary bundle model is quite nebulous and achieving packs with identical geometric parameters will be next to impossible. These factors limit the application of the Washburn method so a new method was developed for estimating the contact angle.

The capillary wetting technique commonly used in the characterization of solid particle surfaces (Malik et al., 1984) was employed with some modifications as described below. The sample container was constructed from a plastic 60-mL syringe barrel trimmed at both ends to create a straight open tube (35 mm i.d., 135 mm long) fitted with a nylon disk (600 cm bubbling pressure) at the lower end, connected to a Mariotte Bottle. Before packing, the inside of the tube was coated with a thin layer of vacuum grease to prevent the fluid from preferentially imbibing between the soil and cylinder wall. About 60 g of soil was uniformly packed using a trimmie tube after which the sample was placed on a vibrating table and shaken for 15 minutes at 150 rpm. The Mariotte bottle was put in place and the balance tared so that liquid uptake could be measured continuously using an electronic balance. Data were collected and displayed graphically using a personal computer interfaced with the balance by an RS232 cable using windmill software (available from www.windmill.co.uk). Rather than fitting the data to the approximate solution offered by the Washburn equation, data are fitted by non-linear regression to the macroscopic energy balance equation (equation of motion), including the effects of gravity and viscosity, for a liquid rising in a vertical capillary. The correct solution for this equation, conditioned on the penetration height at infinite time permits simultaneous calculation of the contact angle and the geometrical parameter. Thus, this method facilitates the determination of contact angle with the need for assumptions of constant geometric parameters between packs or about the wetting characteristics of reference liquids (i.e. $\phi = 0$). Details of the new method, experimental techniques and data analysis are presented by Ward and Gee (2001) and Ward et al (2002).

2.1.5 Critical Salt Concentration for Colloidal Release

Colloidal particles, attached to grain surfaces, are abundant in the subsurface and under specific conditions they can be released from the matrix and subsequently transported with the mobile phase. This mechanism is of potential importance to the transport of cesium-137 and other reactive species that typically adsorb to the solid phase. One of the mechanisms for sudden particle release is a decrease in pore water salt concentration to below the critical salt concentration (CSC), where repulsion forces between fine particles and matrix surfaces exceed binding forces.

Critical salt concentrations are typically determined from column experiments, where a sequence of solutions with decreasing concentrations is applied to the matrix of interest. In CSCs were determined using both batch and column experiments. Two types of sediment were tested: (i) pure, homogeneous silica sand; and (ii) mineralogically heterogeneous sediment, taken from the Hanford formation in southeast Washington. Stepwise decreasing concentrations of sodium nitrate solution were applied until fine particles were released from the sediments, at which point the CSC was determined. In the initial batch experiments particle release due to shear stress and the resulting hydrodynamic forces was high, especially for the Hanford Sediment. Two methods were developed to eliminate this effect: (a) post-experimental correction for mechanical effects; and (b) minimizing shear stress on the sediments during the experiment. CSCs from batch experiments were compared to those obtained from column experiments.

2.1.6 Effects of Fluid Composition on Hydraulic Properties

Soil samples were collected from two 120-cm deep boreholes augered in each caisson (Figure 2). Due to the presence of fist-sized cobbles and low moisture contents, it was difficult to retain all of the sample in the sampler and most samples were therefore collected close to the 20-cm depth. As the samples were unconsolidated and very sandy, cheesecloth gauze was wrapped around one end of each core (the brass ring containing the soil sample) using a rubber band. A nine-point retention curve was obtained for all of the samples using ordinary tap water. From these, 13 samples were selected for two additional drainage curves using that were 17.625 wt. % and 35.25 wt. % of sodium nitrate solution. A nine-point retention curve was then obtained for 13 of those samples using tap water, 17.625 wt. % of sodium nitrate, and 35.25 wt. % of sodium nitrate. This was accomplished using a combination of a hanging column (0-25 cm of solution) and a pressure plate extractor (50-1000 cm of water). The highest concentration was chosen as it is 75% sodium nitrate saturated at 25ºC; the 17.625% concentration sodium nitrate was chosen as it is the median between the two extreme concentrations. The properties of the sodium nitrate solution were taken from Weast (1977). Density was checked in the lab using a volumetric flask and was found to be accurate within 0.5%. For 75% sodium nitrate saturation in water, the concentration is 35.25% by weight, and density is 1273 kg m^{-3}. For a concentration of 17.625% by weight, the density is 1239 kg m^{-3}. The surface tension was measured as 0.08054 N m^{-1} (35.25%) and 0.07519 N m^{-1} (17.625%). The surface tension of pure water at 20ºC is 0.0728 N m^{-1}.

Drainage Curves

A tension table (35 cm x 45 cm x 7 cm deep) was used for the samples and gravimetric moisture content was measured at the following pressure heads: 0 cm, -1 cm, -5, cm, -10 cm, -25 cm of the working fluid. Heads are converted into pressure to account for changes in mass density. Up to 20 samples were measured at a time. The table was slowly filled with solution (tap water, 17.625 wt. % of sodium nitrate, or 35.25 wt. % of sodium nitrate) so that the samples were saturated from the bottom. Solution was added in 1-cm increments over one day to minimize air entrapment. The contact at the bottom of the core and the tension table screen was used as datum to make the head measurements. On reaching steady state (head change < 0.1 ml over 24 hours), each sample was weighed and returned to the tension table. The head was then lowered to the next step and the measurement procedure repeated.

On completion of the –25 cm measurement, the samples were transferred to a pressure plate extractor fitted with a 1-bar porous ceramic plate. The plate was first soaked in an equivalent solution (tap water, 17.625 wt. % of sodium nitrate, or 35.25 wt. % of sodium nitrate) under a slight vacuum for several days. Pressure was delivered to the extractor in increments of 50 cm, 100 cm, 250 cm, 500 cm, and 950 cm of water.. Outflow from the extractor was directed into a burette. Steady state was assumed when the solution level in the burette changed < 0.1 ml day^{-1}. The samples were then weighed in the same manner as with the tension table measurements. The samples were then returned to the pressure plate extractor and the pressure was adjusted to the next step. After the last increment, saturated hydraulic conductivities were measured with water.

Imbibition Curves

The transient method developed by Young et al. (2002) was used to measure the pressure-saturation relationship during imbibition for two samples using tap water and a 35.25 wt. % sodium nitrate solution. The core was placed in a Tempe cell (Soil Measurement Systems, Tucson). A Mariotte system was used to control fluid input to the column. The bottom boundary condition was set at –8 cm of water (-0.8 kPa). With the ceramic plate in place, the core and all of the plumbing was saturated with tap water. The core was then drained for 24 hr by applying a –1 m hanging column of water on the sample. This established an initial saturation condition. The core was then imbibed at –8 cm of water using salt-free water and infiltration was tracked as a function of time using a data logger. After the core was fully saturated it was again drained for 24 hours at –1 m of water head. The imbibition process was then repeated using a 35.25 wt. % sodium nitrate solution. The computer program Hydrus 2D was run in inverse mode to estimate van Genuchten parameters for the resulting two retention curves.

Intrinsic Permeability

Intrinsic permeability under saturated conditions was measured using a constant head permeameter and tap water. The brass ring containing the undisturbed soil sample was placed in a flow cell. The ends of the core were fitted with a layer of silkscreen and a circular, perforated metal disk to retain the soil. An elevated constant head reservoir was of water served as the input; flow was directed downward through the soil with a positive head difference of that was always less than 15 cm (i.e., the gradient was always less than 5 m m^{-1}). For most of the samples, the applied gradient was between 1 and 3 m m^{-1}. The head difference was chosen so that the flow rate through the sample was in the range of 10 to 20 ml min^{-1}. A tube connected to the bottom

port of the cell directed flow into a graduated cylinder for measurement. A "T" was fitted into this tube and a second tube served as a piezometer. The water temperature was maintained between 18º and 21ºC. Head measurements were accurate to ±0.2 cm. Using a stopwatch, the time between known incremental flow volumes was measured. Intrinsic permeability was calculated using properties of fresh water at 20ºC, that is the kinematic viscosity of water was assumed as 1.003×10^{-6} m^2 s^{-1}

Bulk Density

Bulk density was measured after the soils had been oven dried at 105ºC for 24 hours. If the sample did not completely fill the brass ring, the difference in height was measured. The samples were placed in a desiccator to cool to room temperature, and weighed on balance accurate to 0.01 gr. Bulk density was calculated as the mass of dry weight divided by the sample volume.

2.2 Controlled Field Experiments

A series of short-term field tests were conducted at the Hanford site to explore how the enhance vertical transport due to surface tension effects would be manifest in the actual Hanford sedimentary unit. A 25-m long 4-m wide trench was made to a depth of 5 m. The depth was chosen in the field to be sufficient to be in the Hanford unit, below a wind-deposited loess soil. It has been shown that fingered flow is most pronounced in coarser media (e.g., Selker et al, 1992), and so a thick coarse layer was the target of our experimental effort. After excavating through 3 m of soil, an apparently homogeneous layer of over 0.5 m thickness was found. Low flux (0.4l/h for 4 hr) applications of the three test solutions were made using a 10 cm diameter tension infiltrometer every 1.2 m along the width of the trench. Six repetitions were carried out, with a total of 16 successful applications. The plumes were excavated 6-12 hours after application along three vertical sections along the width of the trench, documenting visually the extent of the liquid movement 10 cm in front of and behind the line of application, as well as along the line of application.

A long-term plume migration experiment (LTPM) was initiated by OSU in the fourth quarter of the first year. The primary purpose of the LTPM was to quantify impact of lateral vapor flux on the vertical migration of highly saline solutions. The site was laid out as shown in Figure 2. The site consisted of five 3-m caissons installed to a depth of 3 m. The soil surface was covered to prevent evaporation and unintended infiltration. The experiment included five plumes, each consisting of a dyed saline solution applied over a period of three days via an automated tension infiltrometer. Two of the plumes were distilled water, two of moderate salinity solution (0.5 moles/kg-solution) and two were of high salinity solution (5 moles/kg-solution). The progression of the plumes was continuously monitored with two concentric circles of four 2-m long segmented TDR probes. Readings of moisture content were logged on 30-minute intervals for the duration of the experiment. The experiment was completed with a destructive analysis of each plume in the third quarter of the third year. The position of the dyed plume was documented and the soil was sampled in 0.20-m depth layers with concentric circles of cores taken for the analysis of water content and salinity. The results were expected to be used for validation of the numerical model.

Figure 2. Field Site showing Caissons used in Long-term Transport Experiment.

2.3 Computational Analysis

The scope of this task was the incorporation of new concepts into a three-dimensional numerical simulator. Specific objectives included the incorporation of the appropriate physics to facilitate continuum modeling of gravity fingers; and the development and incorporation of an adaptive gridding algorithm to permit investigation of gravity-fingers over a range of spatial scales. The continuum model used as the basis of this task was the PNNL-developed STOMP (Subsurface Transport Over Multiple Phases). STOMP is a general-purpose multi-fluid flow and transport simulator, developed for modeling waste repositories, geothermal reservoirs, non-aqueous phase liquid contamination and remediation, and the enhanced recovery of petroleum reservoirs (White and Oostrom 2000). The simulator comprises a collection of operational modes distinguishable by the solved coupled flow-and-transport conservation equations. The nonlinear partial differential conservation equations and associated constitutive relations that describe multi-fluid flow and transport through porous media are discretized in space and time and solved iteratively using Newton-Raphson iteration. Spatial discretization occurs via structured grids, yielding sparse linear systems and good computational efficiency. Modeling capabilities include multi-fluid porous media systems, nonisothermal conditions, freezing soils, brines, non-aqueous phase liquids (NAPLs), non-wetting fluid entrapment, kinetic dissolution, hysteretic soil-moisture characteristics, and reactive transport. The simulator has sequential and parallel implementations, and its modular architecture allows for rapid modification and development of new operational modes. The modifications made to the model are described below.

2.3.1 Local Uniform Grid Refinement

The computational burden of simulating multi-component, hypersaline plumes at the field scales in multiple dimensions can be prohibitive. Inherent in this problem are severe differences in length scales associated with finger initiation and growth. This is because processes like gravity-driven fingering typically start at the local scale and ultimately impact transport behavior at the field scale. Because viscous and gravity fingering also have steep spatial and temporal gradients computational techniques that introduce strong numerical dispersion and smear sharp fluid

interfaces are not desirable. Stability conditions associated with common methods require very small time steps, which could result in excessive computational costs for problems like the field-scale infiltration of hypersaline fluids in heterogeneous media. However, for large-scale simulations, it is impossible to accurately represent all the local phenomena by covering the entire domain with a uniform fine grid. The objective of this task was an improved technique for modeling the effects of heterogeneity and gravity fingering in cases of adverse mobility ratios.

To solve the CPU intensive simulations spanning local-scale finger initiation to contaminant distributions in a tank farm, the local uniform grid refinement (LUGR) technique was implemented into PNNL's STOMP simulator. LUGR is an adaptive-grid finite difference solver for time-dependent multidimensional systems of partial differential equations (PDEs) introduced by Trompert et al (1993). The system of PDEs is solved using a method of lines approach. In this approach, the PDEs are first discretized in space, and the resulting ordinary differential equations (ODEs) or differential-algebraic equations (DAEs) in time are solved using a second-order two-step implicit backward differentiation formula (BDF) method. The resulting system of equations created by the BDF method is solved by the user's choice of one of three solvers: (1) bi-conjugate gradient method stabilized (BiCGStab) with ILU preconditioning, (2) generalized conjugate residual orthonormalization, or (3) SPLIB.

The LUGR process consists of eight steps that can be summarized as follows:

1. Start with a uniform base grid
2. compute solution on the base grid
3. compute space monitor based on the curvature
4. where needed, refine by bisection in every coordinate direction
5. obtain secondary grid with ½ cell width of base grid enclosed by the base grid
6. apply the same algorithm on the second grid
7. obtain solution on finest mesh using method of lines
8. space discretization on a 9-point template with second order finite differences
9. solve system of DAEs is solved with an implicit time-integrator (BDF2) with variable stepsizes

2.3.2 Macroscopic Continuum Modeling of Hypersaline Fingers

To investigate the formation and persistence of gravity finger during the infiltration of hypersaline fluids in coarse textured materials, it was necessary develop a method for incorporating the mechanism into a macroscopic-continuum model. Two methods for predicting gravity-driven fingering were implemented for evaluation, (1) the downwind averaging method reported by Nieber (1996), and (2) a new contact-angle hysteresis method developed during the course of this research.

Nieber's (1996) method was originally developed for a two-dimensional form of the Richards equation with hysteretic water retention functions. This approach uses an upstream weighting of the internodal unsaturated hydraulic conductivities to limit dispersion of the steep wetting fronts. An initially dry soil is required and fingers are in initiated as small perturbations in saturation at

the upper boundary. The growth of subsequent fingers is simulated by applying more weight to the downstream node when calculating the internodal unsaturated hydraulic conductivity.

The second method is based on three observations (i) a non-zero contact angles for water on many porous materials; and (ii) the correlation between positive water entry pressures and fingering in hydrophobic soils; (iii) the dependence of water entry pressure on the surface tension and contact angle of the imbibing fluid, and (iv) the insensitivity of the drainage curve to fluid properties. Capillary theory implies that each pore has a characteristic threshold value of suction for liquid entry and that liquid introduced at a suction exceeding that value will not enter the pore. The water-entry suction is calculated for different porous media from thermodynamic relationships taking into account pore geometry. The simplest case of a cylindrical pore is essentially the capillary bundle model commonly used to predict the pressure differential due to capillary forces at the liquid-solid interface during infiltration. The concept of a hydraulic radius was introduced to allow calculation of a pore size parameter for non-cylindrical pores. A critical entry pressure is then defined in terms of the surface tension of the imbibing liquid, the contact angle on the porous medium, and the mean particle size of the porous medium (Ward and Gee, 2002). Setting this critical pressure equal to the first derivative of the imbibition curve for the porous medium and liquid of interest allows determination of the liquid-entry pressure that is not limited by current empirical relationships. This approach has shown that current approaches, which define the liquid entry pressure as twice the air-entry pressure, may hold under very specific conditions.

Full use of this model required a rigorous approach for predicting the surface tension of the concentrated electrolyte mixtures typical of Hanford's Tank wastes. The surface tension model based on the Gibbs thermodynamic method and proposed by Guggenheim and Adam (1933) forms the basis of our approach. It is hypothesized that for a concentrated electrolyte solution and its vapor, there exists a surface layer sandwiched between the bulk liquid and vapor phases. This surface layer is treated as a separate phase whose concentration is related to that in the bulk liquid by an interface parameter (Li et al 1999). This constant is determined from the relationship between published experimental surface tension data and bulk phase concentration. The osmotic coefficients of the bulk liquid and surface phases are calculated by a constrained minimization of the Gibbs free energy using the GMIN model (Felmy, 1995). Details of the surface tension model for single and mixed electrolytes are summarized in Ward and Gee (2001). Results are discussed in Section 5.

The transport of hypersaline fluid in variably saturated porous media occurs over three phases: aqueous, gaseous, and solid. The aqueous phase comprises liquid water, dissolved salt, and dissolved air; the gaseous phase comprises air and water vapor; and the solid phase represents the porous medium. The STOMP simulator was modified to allow solution of the salt mass conservation equations for electrolyte mixtures typically found in Hanford's tanks. Properties that depend on salt concentration, i.e. water-vapor partial pressure; aqueous-phase density; aqueous-phase viscosity; aqueous phase enthalpy; and osmotic pressure were also incorporated into the solution schemes. Calculation of the osmotic pressure required introduction of an osmotic efficiency coefficient to express the degree to which dissolved salt would be effective in reducing the total pressure (Nassar and Horton, 1989). Calculation of this coefficient required estimation of the water film thickness for different Hanford sediments as a function of pressure

head. The required data were derived from a series of half-cell diffusion experiments, which are summarized in Ward and Gee (2002c). The lowering of the vapor pressure due to elevated salt concentration can also induce significant fluxes of water vapor. Such a mechanism could supply hypersaline fingers with moisture from the surrounding porous medium, thereby leading to increased penetration distance. This mechanism was also incorporated into the STOMP code.

3.0 Results

3.1 Infiltration of Hypersaline Fluids in Miller Similar Sands

It should be noted that high concentrations of salts increase the index of refraction of the liquid and consequently affect the saturation values measured using the light transmission method. The magnitude of this effect for a given salt depends on the combination of salt concentration and the degree of liquid saturation and therefore is difficult to accurately correct for. While this perturbation does slightly offset saturation values, and would be of concern if precise mass balance were required, it does not affect the delineation of plumes (geometries and velocities) in this study.

Laboratory experiments demonstrated that high surface tension solutions penetrating into homogenous prewetted unsaturated porous media significantly enhanced vertical fingered flow. From Figures 4 and 5 it is clear that, in all four experiments, the hypersaline solution (*A*) infiltrated faster than *B*, and *B* faster than *C*. Solutions of 5 molal sodium nitrate were found to infiltrate 24-62% faster than pure water, in an unstable, fingered manner (Figures 3 and 4). The first image (time = 0) was taken immediately after the solution application was completed. The infiltrating fluids in these experiments were *A*, *C*, and *B*, from left to right (except Exp. 3, Table 1). The resident fluid was distilled water, *C*.

In natural soils, the occurrence of fingering is still under debate [e.g., *Glass and Nicholl*, 1996]. Natural soils are rarely dry at depth. Also, many coarsely textured natural soils have laterally dominant micro-layering within single strata, and cross bedding with contrasting texture, both due to turbulent and unstable depositional processes. The results presented here suggest that fingering can be enhanced in pre-wetted media when the imbibing solution has elevated surface tension. Moreover, water migration into the saline solution from the surrounding low water content environment, through vapor transport, may further promote fingering [*Weisbrod et al*., 2000a, 2000b].

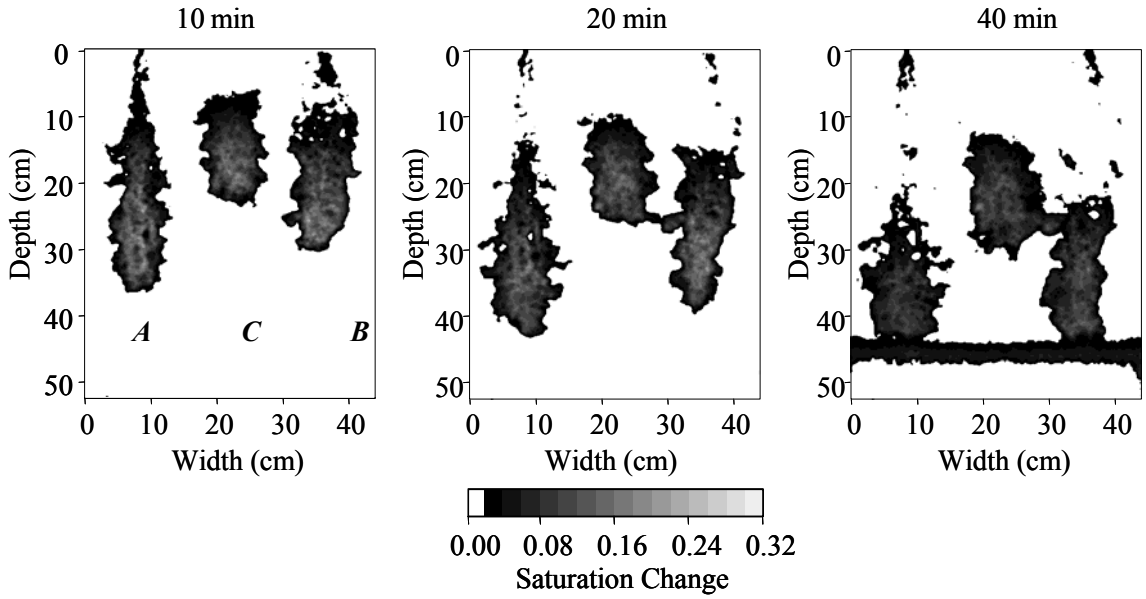

Figure 3. Three frames from Exp. 1. Solutions A, C and B (left to right, respectively) were applied to 12/20 sand prewetted with pure water C. Time from end of application is noted above each frame. The pseudo-colorized gray scale images describe the changes in saturation (ΔS) with respect to before solutions were applied.

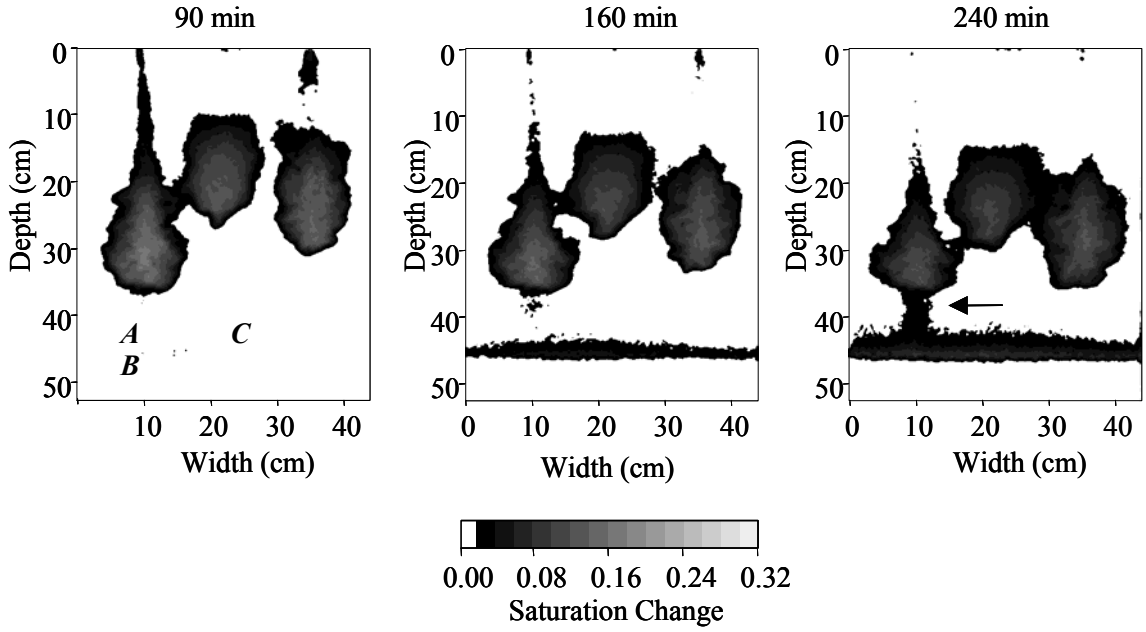

Figure 4. Three frames from Exp. 2. Solutions A, C and B (left to right, respectively) were applied to 20/30 sand prewetted with pure water C. Time from end of application is noted above each frame. The pseudo-colorized gray scale images describe the changes in saturation (ΔS) with respect to before solutions were applied. Arrow denotes the secondary finger.

When the sand was pre-wetted with high-salinity solution, ***A,*** (Exp. 6) it was observed that the pure water, with lowest density and lowest surface tension, infiltrated most quickly, while the methanol solution finger was more rapid than the pure saline solution. The velocities were all within 15%. The higher surface tension of the resident solution appears to have drawn in the lower surface tension solutions more aggressively. Unlike the issue of contact angle, this process is not amenable to a simple force-balance analysis to estimate the expected magnitude of the effect. It is not clear how these processes would effect movement at actual sites, since uniform contamination with a saline solution seems an unlikely description of initial conditions.

It is well known that lowering the surface tension of a fluid by heating or adding surfactants makes it a better "wetting agent" and improves its ability to enter porous media. Conversely, increasing the surface tension (by adding salts) results in more cohesive forces within the fluid

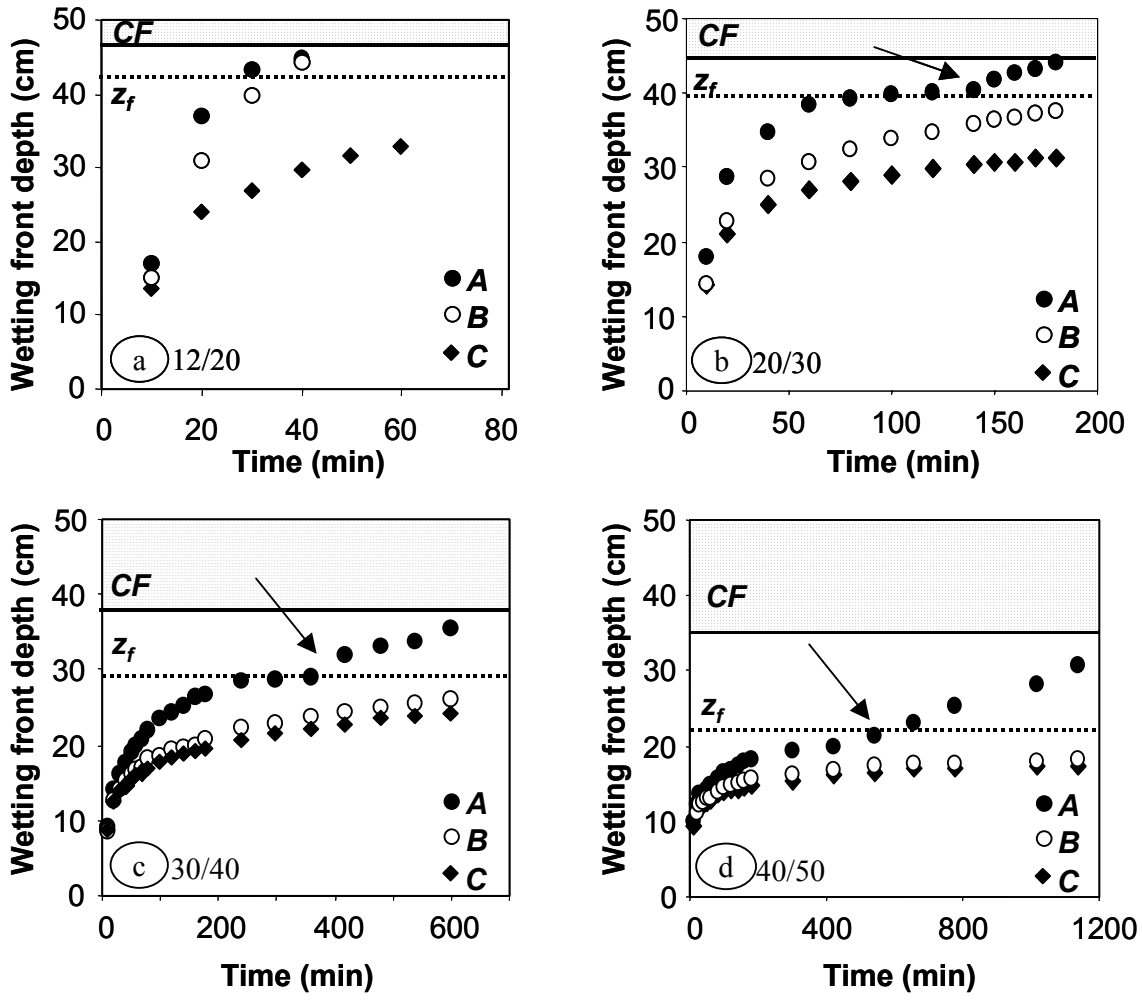

Figure 5. Wetting front depth of solutions *A*, *B*, and *C* for Exp. 1 (12/20), Exp. 2 (20/30), Exp. 3 (30/40) and Exp. 4 (40/50), (a) to (d), respectively. Capillary fringe depth prior to the experiment is noted (as CF, above the solid line) as well as the transition depth where the secondary finger developed (z_f, dashed line).

molecules at the surface, giving rise to an energetic obstacle to imbibition in water wetted media. This latter situation corresponds to the case when the advancing fluid was the saline solution (***A***) and the low surface tension was the resident one (***C***), as well as the initial entry of saline solution in a pristine subsurface environment.

Differences in surface tension between the infiltrating and resident fluids, and consequently the contact angle, had the greatest impact on wetting front velocity and geometry. The gradient in surface energy at the interface between the resident fluid (coating the particles) and the advancing fluid prevented a zero contact angle from forming between the fluids over the relatively short period of contact during infiltration. The magnitude of the resulting contact angle was estimated from the relative surface tension with the understanding that the contact angle is effective across a zone of mixing. Although pure water and saline solutions are typically considered completely miscible fluids, our results suggest that the mixing process is not spontaneous. The micro-scale processes at the interface are not completely understood.

Once the infiltrating solutions reached the depth where resident saturation increased above residual levels, z_f, a visible secondary finger developed at the tip of the plume and the local wetting front velocity increased. The secondary fingers appeared to migrate via film flow rather than isolated pore filling. The accumulation of fluid on top of the capillary fringe without visible contact with the fingertip suggested that film flow occurred through very small changes in water content, below the detection limits of our system ($\Delta S < 2\%$). Further research is needed to quantify the impact of surface tension in different salt solutions and various concentrations as well as to better understand the practical implications of the observed film flow. Also, possible methods to measure the resulting contact angle between solutions need to be investigated. The observed phenomena appear to be influential where infiltrating solutions have high surface tension and should ultimately be incorporated in predictive models.

3.2 Infiltration of Hypersaline Fluids in Hanford Sediments

Laboratory experiments showed that demonstrated that infiltration behavior of the test fluids was strongly influenced by fluid composition and soil type. Infiltration of hypersaline fluids into the grade 30/40 Accusand resulted in finger formation (Figure 6a) even in pre-wetted conditions. Fingering, however, was not observed in the dry or prewetted Hanford sediments (Figure 6b,c,d,e). In contrast, finger formation was observed in a coarse fraction of a Hanford sediments from which the fines had been removed.

The occurrence of fingering in natural soils, other than those that are hydrophobic, is still a subject of intense debate because conditions conducive to fingering are typically absent. The initial moisture content of field soils is usually higher than the air-dry condition used in laboratory studies and thin lenses of in fine-textured materials are typical, even in soils that appear homogeneous at the macroscopic scale. These results show that the infiltration of hypersaline fluids can lead to fingering, even in pre-wetted Accusands. The observation of fingering in coarse fractions of Hanford sediments suggest that this mechanism might bbe of importance under very special circumstances, i.e. homogeneous coarse-textured regions of the profile. However, given the highly stratified nature of the Upper Hanford Formation where most of the wastes currently reside, it is doubtful that this mechanism will be important under typical

field conditions. A more important mechanism may be lateral spreading along textural interfaces and the enhanced migration due to the contribution of osmotically-driven vapor flux.

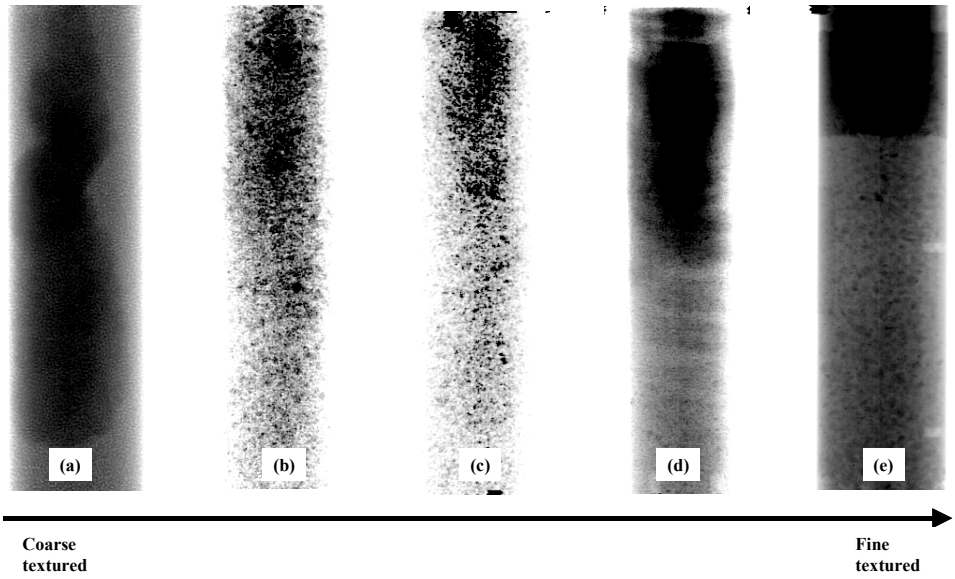

Figure 6. X-ray Microfocus Scans of a Hypersaline Fluid Infiltrating into Porous Media of Various Textures, (a) 30/40 Accusands, (b) through (e), fractions of the Upper Hanford Formation decreasing in texture from coarse sand to silt.

3.3 Contact Angle of Hypersaline Fluids on Silica Sands

Wettability of porous solids, while not obtainable by optical inspection, can be estimated using methods based on capillary models of imbibition. Our methods, both static and dynamic, demonstrated their ability to estimate the contact angle formed by solutions of varying surface tension on silica sands. The contact angle of the imbibing solutions was estimated in both dry and water-wetted sand using an analytical method, based on the Green and Ampt theory, as an effective method for estimating the contact angle of imbibing fluids into dry and pre-wetted sandy soils. The model incorporates the observed lack of complete saturation using the retention/conductivity model of Brooks and Corey (1964) to calculate the effective degree of saturation during imbibition based on the optimized hydraulic conductivity.

The estimated contact angles in the static and dynamic methods were compared for dry sand, showing that dynamic contact angle measured higher for both pure water and 5 molal sodium nitrate imbibition (Table 2). Comparison between the dynamic solution proposed by Rulison (1996) based on Washburn's theory and the Green and Ampt based model for upward imbibition showed that gravity cannot be neglected in coarse porous media such as sand.

Independently measured hydraulic conductivity K_S, which was 1.5 to 20.7 times higher than the fitted conductivity values, was used as a fixed parameter in the Green and Ampt imbibition model so that the model optimized only two parameters (h_f and t_0). With this constraint, the model could not fit the data, suggesting incomplete wetting. The degree of media saturation in

the dynamic tests, calculated using the Brooks and Corey (1964) relationship, ranged from 21% to 30%.

Height of capillary rise plays a major role in pre-wetted sand. The imbibing fluids into the pre-wetted sand columns during static method tests lacked an apparent distinct wetting front. In the static method, calculation of capillary rise was based on the volume of liquid imbibed, yielding smaller capillary rise in the pre-wetted sand than in initially dry sand. However, a greater height of rise in pre-wetted sand is necessary to form the zero contact angle expected for pure water imbibition into water-wetted sand. The infiltration process is apparently dominated by diffuse capillary imbibition and restrictions imposed by the height of the samples. The results of the dynamic imbibition of water-wetted sand revealed apparent contact angles of 2° for water and 21° for 5 molal sodium nitrate, which is very close to the 0° and 25° calculated using Young's equation.

Table 2. Comparison of Contact Angles Derived for Dry Sand using the Static and Dynamic Methods in Dry Sand.

Sand	Solution	Capillary rise, h (in cm)		Pore radius, r (in cm)		Contact angle (in degrees)	
		Static	Dynamic	Static	Dynamic	Static	Dynamic
40/50	n-hexane	6.68	7.71	0.009	0.007	0	0
	Pure water	16.20	13.27	0.009	0.007	23	49
	5 m $NaNO_3$	14.17	13.38	0.009	0.007	23	41
30/40	n-hexane	5.15	6.55	0.011	0.009	0	0
	Pure water	11.48	8.62	0.011	0.009	32	60
	5 m $NaNO_3$	10.04	9.36	0.011	0.009	33	52
20/30	n-hexane	3.68	6.01	0.016	0.010	0	0
	Pure water	8.22	6.43	0.016	0.010	32	66
	5 m $NaNO_3$	7.13	6.41	0.016	0.010	33	63
12/20	n-hexane	2.52	4.85	0.023	0.012	0	0
	Pure water	5.72	5.52	0.023	0.012	30	64
	5 m $NaNO_3$	4.99	4.57	0.023	0.012	31	66

The observed data suggest that the zero contact angle assumption is a poor one for clean dry silica sand. In a dynamic system, the effects caused by gravitational forces cannot be ignored in course porous media. Both methods generated reproducible and reasonably consistent values of contact angle.

3.4 Contact Angle of Hypersaline Fluids on Hanford Sediments

The capillary rise different strengths of salt solutions were studied in columns of repacked Hanford sediments to determine the degree to which solid phase physical properties and the chemical nature of the fluid governs the behavior. The experiments were analyzed using the classical Washburn equation. The Washburn method requires the calculation of a constant

geometry term in order to calculate the contact angle. However, the value of this term varied with the imbibing fluid, which is in violation of the assumptions of the traditional Washburn analysis. Although the Washburn method predicts a linear dependence of the square of the distance of the wetting front on time, this was not the case for the hypersaline fluids. Infiltration kinetics also showed a different sensitivity to the viscosity of the fluids than that predicted by Washburn method. It is hypothesized that at early time, inertial forces control imbibition and the process is characterized by a linear time dependence of the distance to the wetting front (Figure 7). The transition from the inertial to viscous regime predicted by Washburn occurs at a predictable point in time that is a function of the soil type and fluid composition. The deviation appears to be partly due to a dependence of saturation on viscosity (concentration of the fluid).

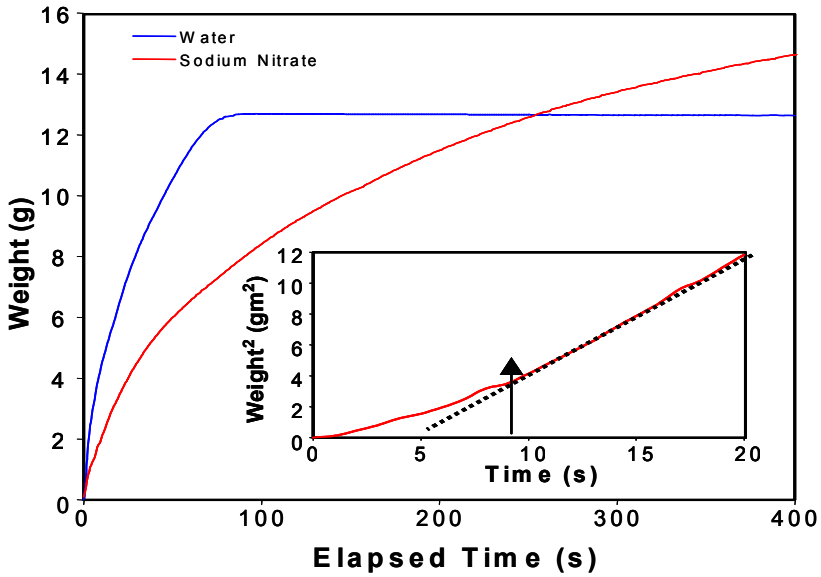

Figure 7. Weight Gain During the Imbibition of Water and 5 Molal Sodium Nitrate in Hanford Sediment. The Inset Shows the Early Time Inertial Region in Contradiction of the Washburn Analysis and its Transition to the Viscous Regime Predicted by Washburn.

More concentrated fluids were more viscous and higher degrees of saturation were observed in the columns exposed to such liquids. The more viscous liquids imbibe at a slower rate resulting in less entrapped air, hence higher saturations. A new method based on complete equation of motion was developed and contact angles were determined by the nonlinear fit of data to the solution. The apparent contradiction of the Washburn method is due to a dynamic contact angle, which varied with the velocity of the wetting front. Calculated contact angles exceeded 80^{o} during the early stages of imbibition, even though values of 0^{o} are typically assumed (Figure 8).

These experiments were first reported by Ward et al (2000) and are the discussed in detail by Ward et al (2002d).

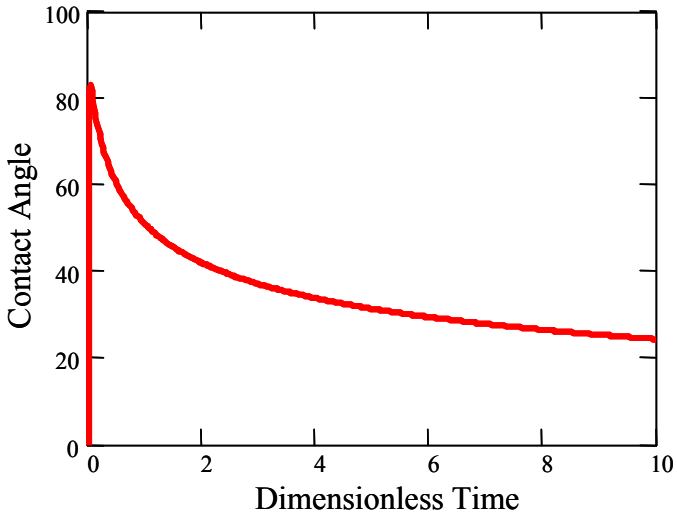

Figure 8. Calculated Contact Angle as a Function of Dimensionless Time During the Imbibition of 5 Molal Sodium Nitrate into an Initially Dry Hanford Sediment.

3.5 Critical Salt Concentration for Colloidal Release

Compared to the commercial sands, the Hanford sediments were mineralogically heterogeneous. The uniformity coefficient of the Hanford Sediment was 3.03, compared to 1.20 for the commercial sand. The mineralogy of the Hanford sediment is dominated by anorthitic plagioclase and ferromagnesian minerals common to basalt (augite and hornblende). The trace (< 10%) clay mineral content is mostly mica (biotite and muscovite), with some smectite (montmorillonite), chlorite, and kaolinite. The clay-sized fraction is typically less than 1%. Particles released from the Hanford sediments are a mixture of mixture of clay and non-clay minerals. Although clays are more abundant in the <5-μm fraction (60-70%), clay minerals accounted 40-50% of the detached particles. The non-clay fraction included quartz, Ca-rich plagioclase, augite, hornblende, traces of K-feldspar, and iron oxides.

In the initial batch experiments particle release due to shear stress and resulting hydrodynamic forces was high, especially for the Hanford sediment. Two methods were developed to eliminate this effect: (a) post-experimental correction for mechanical effects; and (b) minimizing shear stress on the sediments during the experiment. CSCs from batch experiments were compared to those obtained from column experiments. Results suggest that CSCs could be determined successfully by batch experiments. It was also found that both the amount of particle release and the CSC of the Hanford Sediment were an order of magnitude higher than for the Accusand (Figure 9).

Estimated values of fluid shear rate, lift force, and drag force for the batch experiments, assuming a particle size of 2 μm are 6400 s^{-1}, were 3.34×10^{-10} N, and 8.25×10^{-10} N respectively. The short rotation period of the shaker resulted in drag and lift forces in excess of literature values (Bergendahl and Grasso 1998) and clearly affected particle release. Functions were fitted to these data to predict mechanical release and to correct total release during incremental

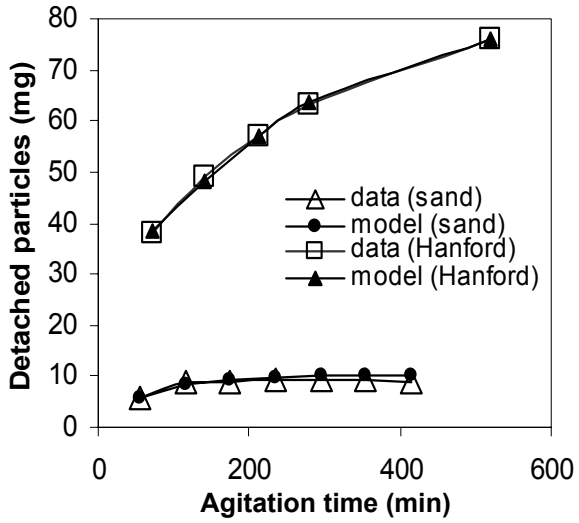

Figure 9. Particle release due to shear stress as a function of shaking time in 0.82 mol/l Sodium nitrate for the Hanford Sediment and in 1.17 mol/l sodium nitrate for the Accusand.

decreases in salinity to determine particle release as a function of CSC alone. The CSC for quartz sand was 0.015-0.032 mol/l sodium nitrate with the amount of chemical release being significantly greater than mechanical release in the vicinity of the CSC. For the Hanford sediment, the mechanical release was in the same order of magnitude as the calculated chemical releases and was a source of error (negative values and inexplicable trends) when correcting for mechanical release. This error limited further use of this procedure for estimating CSC in Hanford sediments. Use of a mesh at the bottom of the column reduced mechanical release to negligible quantities. The range of CSCs derived from the different methods is shown in Table 3.

Table 3. Critical salt concentrations obtained with the three different methods.

Method	Silica Sand	Hanford Sediment
Batch	0.015-0.032 mol/l	0.11-0.17 mol/l
Batch (with mesh)	0.015-0.020 mol/l	0.10-0.11 mol/l
Column	0.028-0.042 mol/l	0.10-0.13 mol/l

Note that the values for the batch experiments are average values, while the column experiment was run without repetition. The limits of the reported ranges are related to the applied concentrations; the CSC must fall between these values. The CSC values found for the Hanford Sediment are larger than most values reported in the literature for well-defined, ideal systems. The presence of montmorillonite in the Hanford sediment might be an explanation for the high CSCs.

Advantages of batch experiments include lower cost, simpler experimental set-up, faster repetitions, and greater control of experimental conditions. The minor amount of particle release

over a range of salt concentrations above the CSC seen in case of the Hanford Sediment would require further investigation to be conclusively explained; however, it is likely the result of the mineralogically heterogeneous nature of both the sediments and the attached particles. Additionally, the high CSC values observed in the case of the Hanford Sediment may be associated with release due to sudden expansion of swelling clays. The total amounts of fines released from the Hanford Sediment were in the order of 3-4 mg/g (~0.3 mg/g for the Silica Sand). The large amount of released particles has a potential importance for either change in sediment permeability (clogging of pores due to fines accumulation), or for migration of contaminants cesium-137 with high affinity to the solid phase. At the Hanford Site naturally borne particles could be detached from the sediment matrix when salinity falls below the CSC due to the dilution of the contaminant plume. These fines may then be transported through the layers of coarse sediments. The relatively high CSC value and the minor particle release observed at salinities above the CSC suggests the presence of mobile particles even at relatively high salt concentrations. This is especially important under the aspect of colloid facilitated contaminant transport. The complex interactions between final salinity, gradient in salinity, hydrodynamic forces, availability and mineralogy of particles on the matrix surfaces all have an impact on particle release and are often difficult to distinguish. The method described here could facilitate a more detailed study of these influences and their relative importance for particle release from sediments as a result of changing salinity.

3.6 Effects of Fluid Composition on Hydraulic Properties

The capillary pressure–saturation curves for eleven of the thirteen samples are presented in Figure 10. A spreadsheet program was written to compute the van Genuchten parameters α, n, m, θ_r, and θ_s to the data (Table 4) using nonlinear least squares optimization (Wraith and Or, 1998). Fits to the data result in residual moisture contents ranging between 0 and 0.14. Volumetric moisture content at saturation is estimated as being between 0.37 and 0.60, with the mean around 0.40. Sandy samples such as 5a-27, 5a-80, and 5a-83 show a very characteristic change in air entry pressure as a function of solution concentration. Results show that the air entry pressure increases with sodium nitrate concentration, hence with increasing surface tension. The increase in surface tension from water to 35.25 wt. % sodium nitrate is about 13%; the air entry pressure for the two solutions are on the order of -700 to -800 Pa for tap water and -3000 to -5000 Pa for sodium nitrate. For pressures more negative than approximately -50,000 Pa, the data nearly universally converge to the same curve and the curves behave similarly.

Table 4. Fitted van Genuchten's n and α, Residual and Saturated (volumetric) Moisture Contents, Intrinsic Permeability, and Bulk Density for each of the 13 samples.

Sample I.D.	n	m	α Pa^{-1}	θ_r	θ_s	k m^2	ρ_b gr cm^3
1a-120	0.6140	1.0000	6.0×10^{-5}	0.00	0.54	4.8×10^{-13}	1.2
1b-60	0.5088	1.0000	1.1×10^{-4}	0.00	0.60	7.1×10^{-13}	1.2
1b-110	1.0463	1.0000	4.1×10^{-4}	0.12	0.53	1.1×10^{-12}	1.4
2a-118						6.5×10^{-12}	
4a-20	0.9547	0.3238	2.7×10^{-4}	0.07	0.54	2.6×10^{-12}	1.4
4b-1						3.0×10^{-12}	
5a-2	0.9427	0.2305	3.7×10^{-3}	0.00	0.43	5.3×10^{-12}	1.5
5a-27	30.7880	0.0422	2.3×10^{-3}	0.14	0.53	1.6×10^{-11}	1.6
5a-80	29.9995	0.0225	2.4×10^{-3}	0.05	0.44	8.2×10^{-12}	1.7
5a-83	1.0000	2.7982	2.4×10^{-4}	0.07	0.46	9.2×10^{-12}	1.4
5a-100	19.9988	0.0187	2.6×10^{-3}	0.01	0.40	1.3×10^{-12}	1.5
5b-2	8.9942	0.0105	2.5×10^{-2}	0.00	0.37	3.8×10^{-13}	1.3
5b-40	8.9997	0.0360	1.3×10^{-3}	0.00	0.48	1.0×10^{-12}	1.2

Bulk density ranged from 1.2 to 1.7 g cm^{-3}. The lowest bulk densities are for the samples with the most sand; when coring, some of the samples were not cohesive enough to remain in the sampler. Some of the sample may have been comprised of material that fell from above the sample point into the borehole. More competent samples with higher amounts of silt and clay have higher bulk densities, in the range of 1.5 to 1.7 g cm^{-3}. Relative permeability values range between 10^{-12} and 10^{-13} m^2.

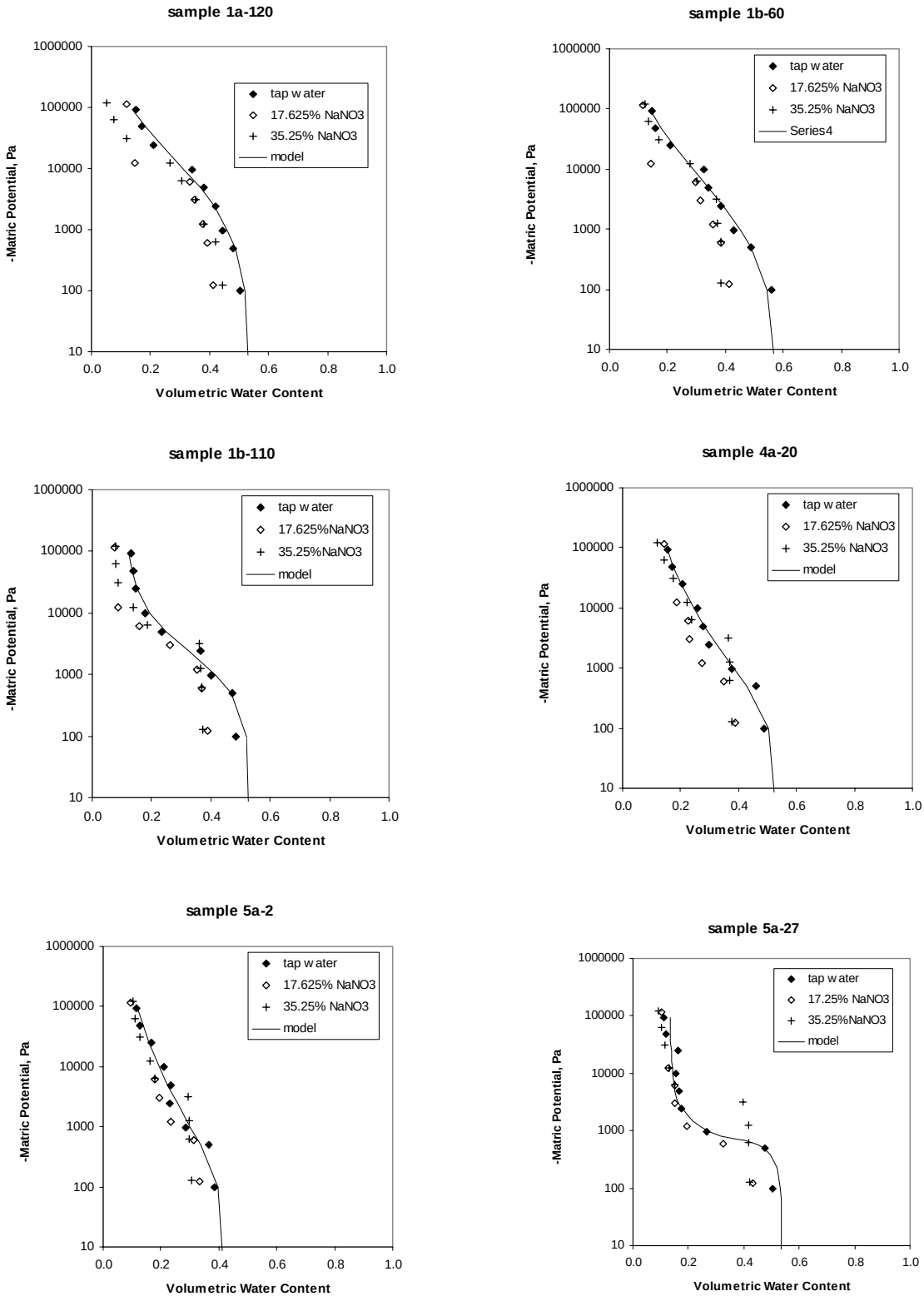

Figure 10. Retention Curves Measured Drainage for the 6 of the 13 samples. Fitted van Genuchten parameters are summarized in Table 5.

3.7 Controlled Field Experiments

The field experiments were intended to explore the transport of the hypersaline plume at two time scales, a reflection of the different time scales at which initial imbibition and vapor migration processes proceed. Although laboratory experiments demonstrated that elevated surface tension of imbibing solutions can enhance vertical fingered flow, field tests showed fingered flow behavior was overwhelmed by the variability in depositional sediment texture. In the field, plumes were predominantly lateral in extent with average width to depth aspect ratios of 3.6 (Figure 11).

Figure 11. Typical Plumes Observed in the Field Experiment, (a) (b) and (c) show the extreme inter-bedding effects within the coarse materials, (b) the left most plume is pure water, the center 5 M NaCl, and the right 5M NaCl plus 2% methanol. The sharper, more laterally pronounced character of the saline plume was observed in almost all cases, with the methanol and water plumes generally being less sharply defined and with less vertical extent, and (d) illustrates the effect of a fine-sand layer, in which all flow is limited to the fine with complete capillary block to entry in the coarse sands.

This was despite our best efforts to avoid the prominent horizontal banding between layers of distinct texture. The horizontal movement is likely due to capillary barrier effects (Kung, 1990; Ross, 1991, Selker, 1997) caused by pore-scale anisotropy. This was demonstrated by sampling within and below wetted lateral bands. Sieve analysis of 12 such sample pairs showed that the ratio of mean particle diameter (d_{50}) above and below the wetted band was 0.797 (s.d.=0.144) which with $p=5x10^{-7}$ is less than 1, indicating a fine-over-coarse banding within the unit. These capillary effects overwhelmed the surface tension and density effects that were expected to generate vertically extensive with plume geometry. In fact the hypersaline plumes appear to have been slightly wider than those of other solutions. Because fingered flow is only prominent in coarse sands, and such coarse sands are deposited in high-energy geologic processes that tend to be sporadic, that fingered flow may typically be a second order process in natural media. These tests show that fingered flow behavior was overwhelmed by the variability in depositional sediment texture.

The observed lateral flow was likely a lower bound on what would be seen under actual spills in the Hanford unit since care was taken to avoid the pronounced fine/coarse bedding features of the unit. Figure 12 shows the distribution of selected radionuclides in the vadose zone beneath BX Tank Farm as identified by spectral gamma logging. At this site, contact between the coarse-grained and fine-grained facies of the Upper Hanford Formation occurs at a depth of 55 ft (16.8 m) and the fine-grained sediments appear to play a major role in transport. Much of the ^{238}U, (the most mobile of the detected radionuclides), ^{60}Co, ^{125}Sb, and ^{154}Eu contamination is in the eastern region and appears to have emanated from tanks BX-101 and BX-102 (DOE-GJPO, 1998). Thus, contaminants appear to have migrated laterally more than 100 ft (30.5 m) within the fine- grained sediments. Investigation of the 1973 leak from the single-shelled tank 241-T-106 also showed significant lateral fluid movement and isopleths of ^{106}Ru suggested a ratio of lateral to vertical spreading in excess of 4:1 (Rouston et al., 1979).

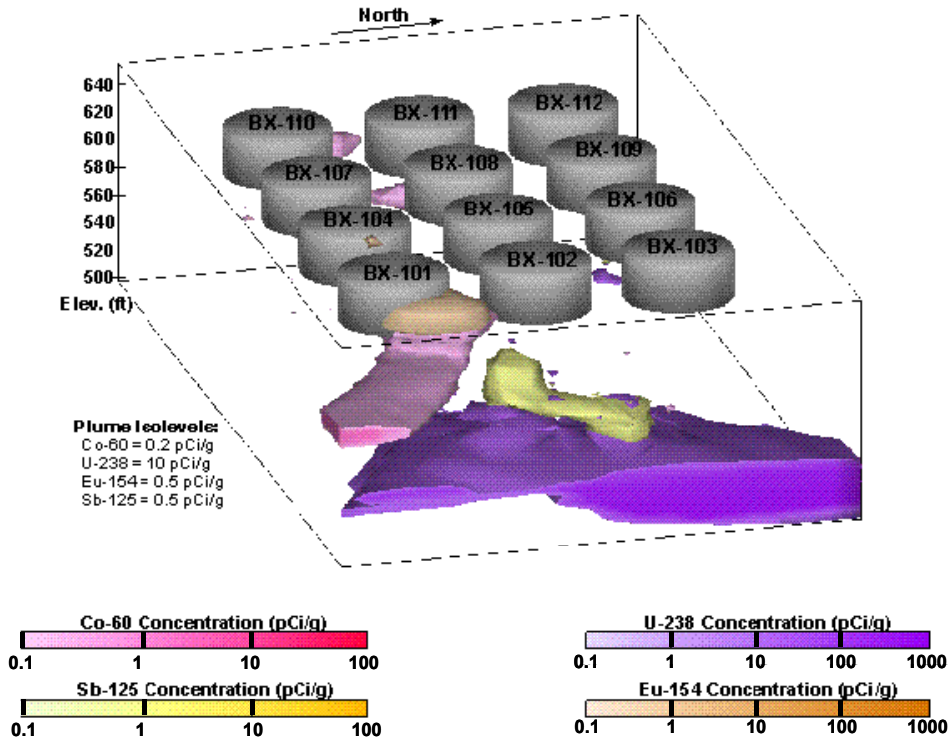

Figure 12. Visualization of the ^{60}Co, ^{238}U, ^{154}Eu, and ^{125}Sb Contamination in Hanford's BX Tank Farm Viewed from above the Tanks and from the Southeast showing extent of lateral spreading of a leaked plume.

Thus, it seems likely that slowly leaked materials would flow along the fine layers that act as capillary barriers. In such a configuration lateral transport would be further driven by water vapor delivered from the coarse materials above and below the band of transport. In both of the laboratory and field studies, water vapor was drawn from the pristine local media and condensed in the contaminated area due to vapor pressure lowering. Given the efficiency of such vapor delivery down to concentrations on the order of 0.01 those seen in leaked wastes (Kelly and Selker, 2001), this process could lead to much greater lateral spreading than would be expected from a simple analysis of the volume of waste entering the environment. The increase in

contaminated liquid would be expected to drive further either lateral or vertical migration, creating a self-propagating plume in the unsaturated zone of ever decreasing concentration. The concentrated solutions leaked at the Hanford site are dominated by the exchangeable hydrating cation, sodium and the sequence of high to low contaminant concentration developed by this vapor stripping process should be expected to lead to defloculation of colloids and facilitated transport of chemicals bound to such colloids (Blume, 2001).

The long-term plume migration experiments were initiated by OSU in the fourth quarter of the first year. An initial three-week field exercise focused on initiation of the LTPM, site characterization and sample collection, and exploratory short-term infiltration experiments. The second two-week effort, in June of 1999, focused on spatial variability of short-term infiltration processes. The final three-week field campaign focused on the destructive evaluation of the long-term vapor migration experiments. The LTPM was monitored continuously through the third quarter of the third year and was destructively evaluated near the end of the project. However, these data have not been analyzed.

However, the findings of the small-scale field experiments are of particular relevance to describing current distributions of contaminants and predicting the future behavior of such plumes in response to remediation options that may leave waste in the ground. The effects of strong anisotropy have proven quite difficult to predict at the Hanford Site with current conceptual models. Prediction error is increased if analyses focus simply on the volume of waste leaked into the soil. Revisions of the conceptual models must therefore account for these mechanisms if realistic predictions of subsurface contaminant behavior are to be made.

3.8 Computational Analysis

The STOMP simulator comprises a collection of operational modes distinguishable by the solved coupled flow-and-transport conservation equations. The simulator has sequential and parallel implementations, and its modular architecture allows for rapid modification and development of new operational modes. During the course of this study, STOMP was modified to include local uniform grid refinement to allow investigation of the behavior of hypersaline fluids in heterogeneous porous media. The simulator was also updated to include other theories developed to describe the thermodynamic dependence of surface tension on fluid composition concentrated electrolytes; the nonlinear dependence on salt concentration of water-vapor partial pressure; aqueous-phase density; aqueous-phase viscosity; aqueous phase enthalpy; and osmotic pressure.

3.8.1 Local Uniform Grid Refinement

A numerical method has been developed and implemented for accurately solving the problem of two-phase, miscible flow through heterogeneous porous media. The method is based on and gridding algorithm and uses local uniform grid refinement. The grid consists of rectangular blocks which can iteratively be refined in areas with steep pressure and wetting fronts, concentration fronts and large permeability contrasts (Figure 13). The LUGR method proved to be a robust and efficient method with respect to the location of the refined grids, especially when a very fine grid was required in part of the domain. The technique saves as much as an order of magnitude in computational time on 3D systems of PDEs.

The computational burden associated with a LUGR solution is split between the base grid calculations, the fine grid calculations, and the overhead associated with error estimation, subgrid generation and grid communication. Simulations with STOMP show that LUGR achieves results similar indistinguishable from those obtained using a uniform fine grid at for a fraction of CPU cost. The real savings lie in the simulation of computationally intensive flow and transport in strongly heterogeneous porous media. In most cases, the cost of simulation with a uniform fine discretization would be prohibitive.

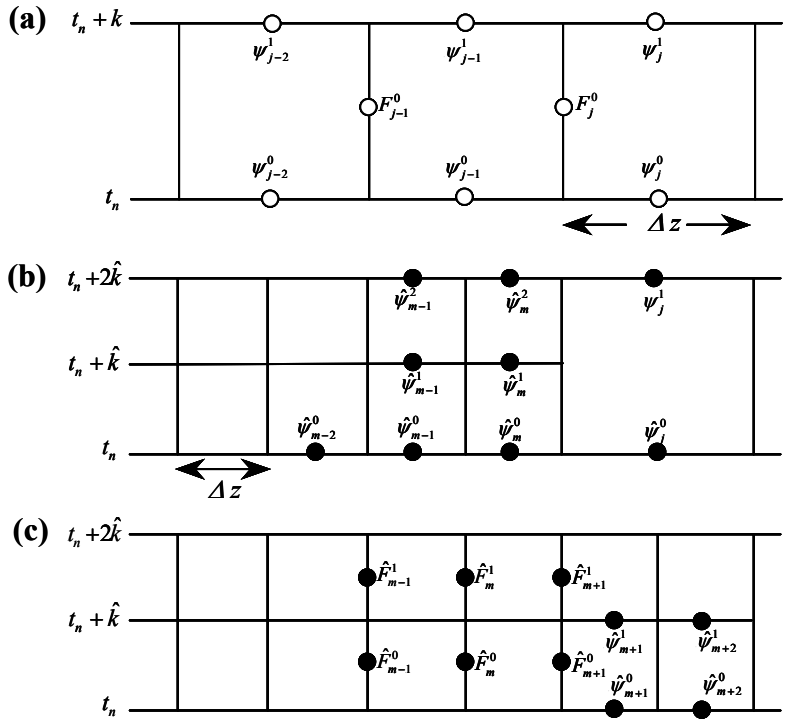

Figure 13. Space-time schematic of LUGR for a one-dimensional case showing value of ψ and fluxes F, (a) coarse grid, (b) overlay of fine grid, grid interface and values of $\hat{\psi}$, and (c) required flux values, $\hat{F}$ for fine grid.

The method introduces little or no numerical dispersion and can be used with large time steps when the physics of the problem allows. The method has been applied to stable and unstable displacement problems in multiple dimensions (Ward and White, 2002).

3.8.2 Macroscopic Continuum Modeling of Hypersaline Fingers

Theoretical analysis and model simulations with the downstream averaging method show that finger formation and persistence results from hysteresis in the water retention function with the finger characteristics being dependent on the shape of the main wetting and main drainage branches of the hysteretic function. Similar to the results of Nieber (1996), it was shown that small perturbations in saturation would grow into gravity finger in initially dry porous media in which the water-entry pressure on the main wetting curve was less than the air-entry pressure on

the main drainage curve. Subsequent drainage and re-wetting of the porous medium resulted in the formation of a finger at the location of the previous finger. However, if the water-entry pressure on the main wetting curve exceeded the air-entry pressure on the main drainage curve, infiltration was governed by diffusion and fingers failed to form. Fingers were characterized by unexplainable profiles, even in statistically homogenous media and appeared insensitive to fluid properties (Figure 14).

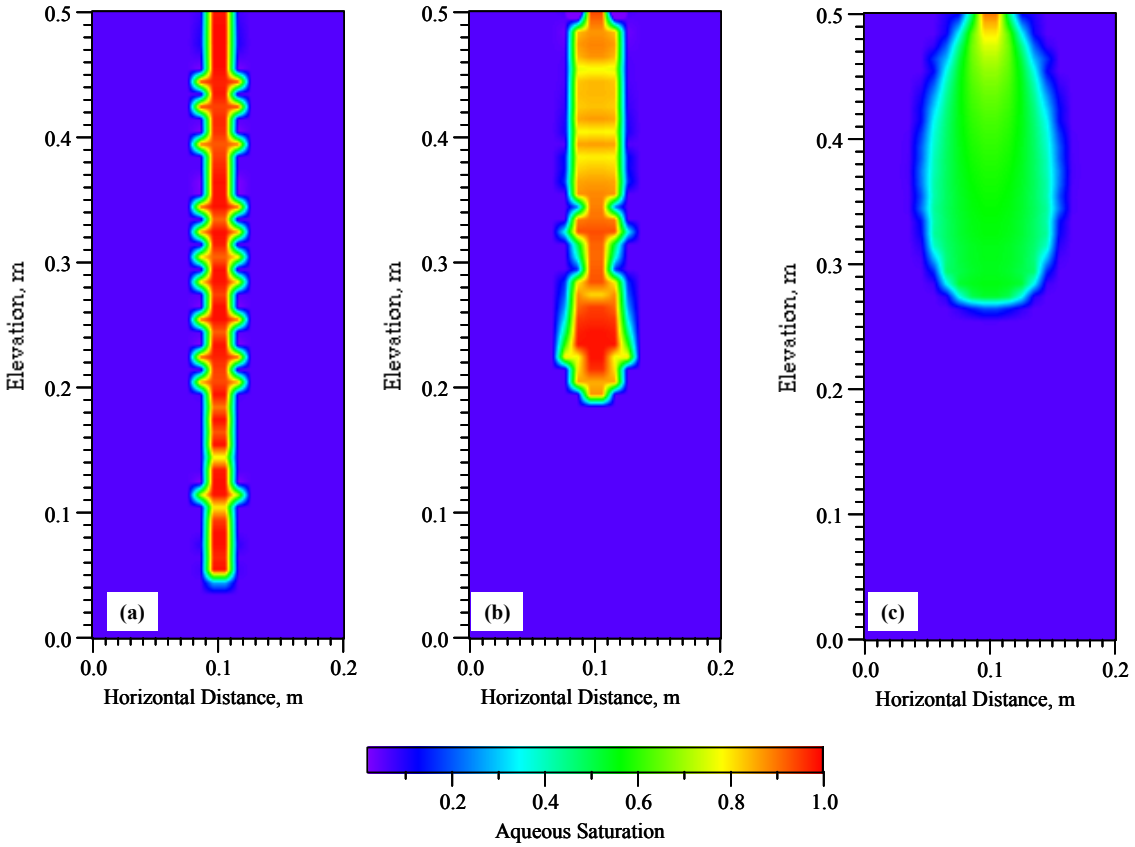

Figure 14. Simulations of Fingering of Hypersaline Fluids in a 2-D Domain of 30/40 Accuasand. (a) Hysteretic Medium and Downstream Weighting (Weighting Factor = –0.8); (b) Nonhysteretic Medium with Downstream Weighting (Weighting Factor = –0.8) (c) Nonhysteretic with Finely Discretized Domain.

These observations led to an in-depth analysis of the mechanism and algorithms (Ward et al, 1999). Results of this analysis show that gravity-fingering in initially dry porous media, as simulated by the downstream averaging procedure, occurred as a consequence of oscillations in the numerical solution due to truncation error compounded by over-saturation at the finger tip. As shown in Figure 14, previously unexplainable artifacts in the fingers and the fingers themselves could be eliminated through very fine discretization of the simulation domain and the use of nonhysteretic water retention functions (Ward et al, 1999, 2000). These results raises questions about the validity of Nieber's (1996) method and its ability to capture the physics governing the process.

Modification of the description of the water retention function to include the dynamic and contact angle described in Section 5.4 allowed the incorporation of a contact angle hysteresis into the water flow equation. The critical liquid entry pressure and initial contact angle were allowed to vary with fluid composition while drainage processes were treated as being independent of contact angle. Setting this critical pressure equal to the first derivative of the imbibition curve for the porous medium and liquid of interest allowed determination of the liquid-entry pressure that is not limited by current empirical relationships (wetting water entry equal twice the air entry pressure). This approach has shown that current approaches, which define the liquid entry pressure as twice the air-entry pressure, may hold under very specific conditions. Incorporation of this theory into the STOMP simulator has led to the successful simulation of fingering without the limitations of the Nieber (1996) method (Figure 15).

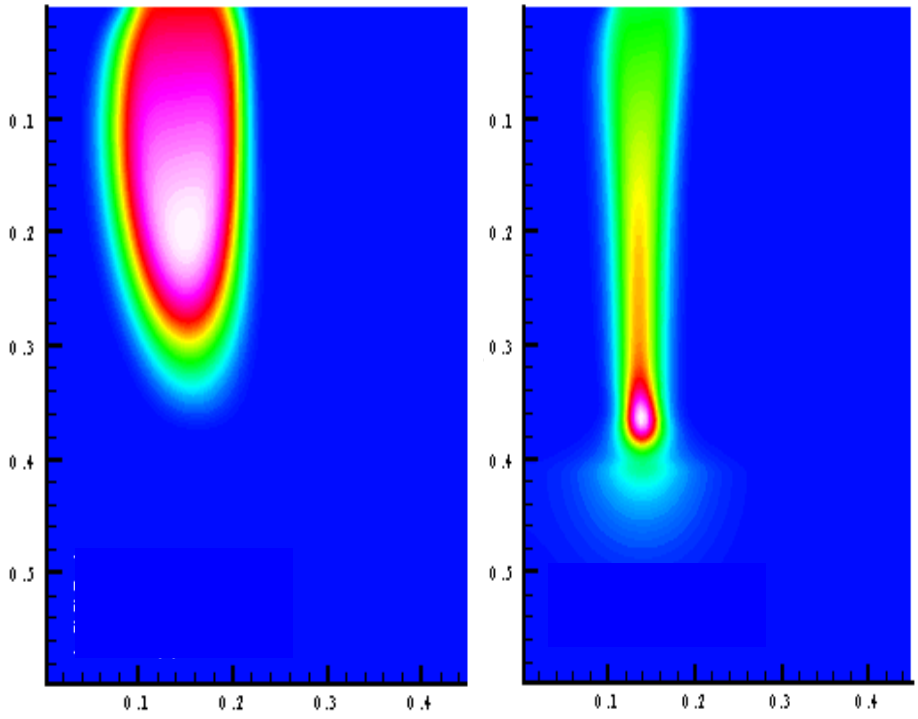

Figure 15. Simulations of Hypersaline Fluids in a 2-D Domain of 30/40 Accusand Showing the Effects of Surface Tension and Contact Angle Hysteresis (a) No Effects, (b) surface tension and contact angle effect effects.

Full use of this model required a rigorous approach for predicting the surface tension of concentrated electrolyte mixtures typical of Hanford's Tank wastes. A model, based on the theory of Guggenheim and Adam (1933) was implemented to permit calculation surface tensions for mixtures of electrolytes. Osmotic coefficients of the bulk liquid and surface phases are calculated by a constrained minimization of the Gibbs free energy using the GMIN model (Felmy, 1995). Investigation of the properties of tank wastes simulants show that the sodium nitrate solutions, commonly used in the laboratory, and sodium chloride solutions, typically used in numerical simulations to represent tank waste fluids, are inappropriate with respect to the predicted water activities and osmotic pressures. Laboratory tests and model simulations with mixed salts show significant vapor flux and soil dessication, even when salt is not in contact with

soil. This phenomenon could therefore affect in-tank moisture balance. However, use of single salt underestimates the effect of the osmotic potential on vapor flux primarily because of an underestimation of the water activity of the waste. Figure 16 shows a plot the change in water content along s5-cm columns packed with Hanford sediments after being exposed to a tank waste simulant and 5 molar sodium nitrate. The salts were placed at one end of the column and the system allowed to equilibrate for different periods. Even with a higher initial water content (2o voil. %), the soil exposed to the tank waste simulant showed a more dramatic change in moisture along the length of the column due to vapor flux.

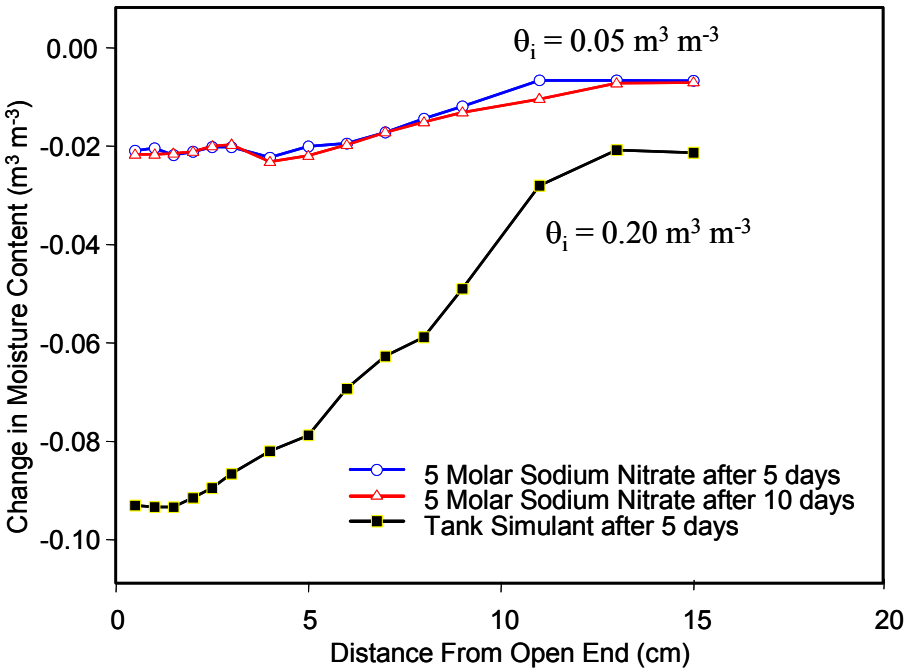

Figure 16. Change in Soil Water Content at 5 and 10 days after Soil Columns were Incubated with 5 M Sodium Nitrate and a Tank Waste Simulant at Different Initial Water Contents

The predicted (using this model) and measured relative humidity of a typical tank waste was 0.47 at a moisture content of 50 vol. %, compared to a value of 0.87 for a 5 molar sodium nitrate solution. It is therefore important to choose fluids that are representative of actual tank waste when simulating potential effects of physical and chemical properties. The STOMP code has been modified to simulate these effects for salt mixtures.

4.0 Relevance, Impact, and Technology Transfer

As recently pointed out by The National Academy of Sciences, the significant knowledge gap in conceptual model development is partly responsible for the discovery of subsurface contamination in unexpected places (National Academy of Science, 2000). Inadequate conceptualizations limit, not only the understanding of long-term fate and transport, but also the selection and design of remediation technologies often leading to the costly over-engineering of

such technologies. The DOE could easily spend billions remediating a site or excavating contaminated sediments if it the amount of soil to be treated or the lateral and vertical extent of contamination are not known *a priori*. This study resulted in a step change in the conceptualization of the subsurface transport of tank wastes at the Hanford site through the following:

(a) The integrated study reported here addressed the fundamental problem of how to describe and predict the migration of hypersaline fluids in unsaturated porous media. It specifically addressed well acknowledged limitations in the conceptual models and theory currently used to predict migration of high ionic strength or hypersaline wastes leaked from high-level waste tanks.

(b) Results show that the interaction between chemical properties of imbibing fluids and the physical properties of the solid phase are important to predictions of fluid migration. It has been shown that hysteresis in the contact angle is one approach for capturing the physics of flow of these fluids.

(c) The results of this study demonstrated the potential for the formation and persistence of fingers due to high salinity, even in pre-wetted porous medium

(d) This study confirmed the desiccation of soils near hypersaline fingers and soil zones due to enhanced vapor flux in response to the osmotic potential gradient

(e) Traditional transport theory has been modified to explain migration of hypersaline contaminant plumes thereby creating a tool that DOE can use for risk assessment, prediction, and evaluation of different remediation strategies

(f) The developments resulting from this study are already being applied at Hanford in the description and prediction of waste migration in the SX Tank Farms and in the groundwater/vadose zone integration project. Under the science and technology component of this project, a team of scientists from PNNL, LANL, LBNL, and LLNL are working on identifying and quantifying appropriate representations of subsurface processes controlling transport in vadose zone sediments with waste that is high in temperature, density, viscosity, ionic strength, and pH. The findings of this project have also contributed to the development of inverse methods for estimating field-scale hydraulic properties under the integration project.

The numerical techniques and models resulting from this work are available for public use. The STOMP simulator is available for download at http://www.pnl.gov/etd/stomp.

5.0 Project Productivity

Most of the tasks originally proposed for this study were successfully completed during the four period. The results summarized in previous sections have provide valuable insight into processes that were traditionally neglected and have led to the identification of mechanisms that were never

taken into consideration when modeling tanks waste migration. Some of the physical mechanisms, e.g. contact angle hysteresis, and fluid dependent water entry pressures were not anticipated and are somewhat more complex than current approaches. Work will continue in these areas as we strive for better predictive capabilities for DOE's waste sites.

During this project, we encountered obstacles related to funding arrangements and data sharing agreements made during preparation of the proposal and in the planning stages of the project. These obstacles affected the project schedule and resulted in the elimination of tasks like the field-scale infiltration test at Hanford and the intermediate-scale fingering experiments in Hanford sediments. At the same time, tasks that were not initially proposed e.g. colloidal release and transport were introduced at the expense of originally proposed tasks. Nevertheless, the theory and methodology developed in this study provides the first consistent approach to macroscopic description of fingering due to elevation in surface tension. The theoretical and computational capabilities developed in this project is already being brought to bear of other subsurface transport problems at Hanford and other DOE sites.

6.0 Personnel Supported

Dr. Anderson Ward, Pacific Northwest National Laboratory (PI)
Dr. Glendon Gee, Pacific Northwest National Laboratory (Co-PI)
Dr. Mark White, Pacific Northwest National Laboratory
Nino Aimo, Pacific Northwest National Laboratory
Dr. John Selker, Oregon State University (Co-PI, collaborator)
Dr. Noam Weisbrod, Oregon State University (postdoctoral associate)
Mark Rockhold, Oregon State University (Ph.D Student)
Mike Niemet, Oregon State University
Theresa Blume, Oregon State University (MS Student)
Thomas McGinnis, Oregon State University (MS Student)
Dr. Scott Tyler, Desert Research Institute/ University of Nevada at Reno (Co-PI, collaborator)
Dr. Clay Cooper, Desert Research Institute (postdoctoral associate)

7.0 Publications

Blume, T., N. Weisbrod, and J.S. Selker. 2002. Determination of Critical Salt Concentrations For Particle Release in Homogeneous Silica Sand and Heterogeneous Hanford Sediments. (*In Review*)

Blume, T. 2001. Critical Salt Concentrations For Particle Release in Homogeneous Silica Sand and Heterogeneous Hanford Sediments. MS Thesis, Oregon State University

Kelly, S.F, and J.S. Selker. 2001. Osmotically driven water vapor transport in unsaturated soil. Soil Sci. Soc. Am. J. 65:1634-1641.

McGinnis, T. 2001. "Determining Contact Angle of Solutions with Varying Surface Tension on Dry and Pre-wetted Silica Sands." MS Thesis Oregon State University Bioengineering.

McGinnis, T, J.S. Selker, and N. Weisbrod. 2002. “Determining Contact Angle of Solutions with Varying Surface Tension on Dry and Pre-wetted Silica Sands.” (In Review)

Niemet, M.R., and J.S. Selker. 2001. A new method for quantification of liquid saturation in 2D translucent porous media systems using light transmission, Adv. Water Resour. 24, 651-666.

Niemet, M. R., M.L. Rockhold, N. Weisbrod, and J. S. Selker. 2002. The relationship between gas-liquid interfacial surface area, liquid saturation and light transmission (In Review).

Ward, A.L., and G.W. Gee. 1999. “Numerical Analysis of Wetting Front Instability Induced by the Infiltration of Highly Saline Fluids.” Agronomy Abstracts, pp 186. American Society of Agronomy, Madison, WI.

Ward, A.L., and G.W. Gee. 2001. A Gibbs Thermodynamic Model for Predicting the Surface Tension of Hypersaline Fluid Wastes (In Review)

Ward, A.L., and G.W. Gee. 2001. “The Influence of Fluid Interfacial Characteristics on the Wetting of Mineralogically Heterogeneous Porous Media.” (In Review)

Ward, A.L., G.W. Gee, and C.S. Simmons. 2002. “The Concept of a Dynamic Contact Angle to Describe the Capillary Rise of Hypersaline Fluids.” (In Review)

Ward, A.L., and G.W. Gee. 2002. “Prediction of Liquid-entry Pressures on the Basis of Fluid Composition.” (In Review)

Ward, A.L. and M.D. White. 2002. “Continuum-scale Modeling of Hypersaline Fingers in Unsaturated Porous Media With an Adaptive-Grid Method.” (In Preparation)

Ward, A.L., M.D. White, G.W. Gee, N. Weisbrod, J.S. Selker, and C. Cooper. 2000. Incorporating the Effect of Fluid Constitution on Surface Tension and Equilibrium Contact Angle into Predictions of Hypersaline Fluid Migration in Unsaturated Soils, EOS Trans. AGU, 81 (48), Fall Meet. Suppl.

Ward, A.L., and G.W. Gee. 2002. Prediction of Liquid-entry Pressures on the Basis of Fluid Composition. (In Review)

Ward, A.L. 2002. Concentration Effects on Wetting Coefficients and Capillary Pressure-saturation Functions of Porous Media. (In Preparation)

Ward, A.L. 2002. Continuum-scale Modeling of Hypersaline Fingering in Unsaturated Porous Media. (In Preparation)

Weisbrod, N., M. Niemet, M. Rockhold, T. McGinnis, and J.S. Selker. 2001. Infiltration of Saline Solutions into variably saturated porous media. (In Review)

Weisbrod, N., T. McGinnis, M. Niemet, and J.S. Selker. 2000. Infiltration Mechanisms of Highly Saline Solutions and Possible Implications for the Hanford Site, EOS Trans. AGU, 81 (48), Fall Meet. Suppl.

Weisbrod, N., M.R. Niemet, and J.S. Selker. 2000. Imbibition of saline solutions into dry and prewetted media (In Review).

Weisbrod, N., M. R Niemet, T. McGinnis, and J.S. Selker. 2002. Vapor Flow in the vicinity of saline plumes: homogeneous and layered unsaturated porous media. (In Review)

8.0 Interactions

During the course of study, the research team made several presentations at national and international meetings. These included:

Ward, A.L., and G.W. Gee. 1999. "Numerical Analysis of Wetting Front Instability Induced by the Infiltration of Highly Saline Fluids." Soil Science Society of America Annual Meeting, Salt Lake City, Utah.

Ward, A.L., and G.W. Gee. 1999. *"Understanding the Transport of High Salinity Tank Wastes Through the Vadose Zone,"* Presented to Hanford's Expert Panel, May, March, 1999, Richland, Washington.

Ward, A.L., and G.W. Gee. 2001. "Vadose Zone Transport Field Studies at the Hanford Site, NGWA National Groundwater Well Association Annual Meeting, February 2001,Portland, Oregon.

Ward, A.L., and G.W. Gee. 2000. *"Factors Affecting the Transport of Hypersaline Fluids Through the Vadose Zone,"* Presented to The Hanford Site Technology Coordination Group, Richland, Washington.

Ward, A.L., M.D. White, G.W. Gee, N. Weisbrod, J.S. Selker, and C. Cooper. 2000. Incorporating the Effect of Fluid Constitution on Surface Tension and Equilibrium Contact Angle into Predictions of Hypersaline Fluid Migration in Unsaturated Soils. AGU Fall Meeting, San Francisco, California.

Ward, A.L., G.W. Gee, J.S. Selker, and C. Cooper. 1999. Rapid Migration of Radionuclides Leaked from High-Level Water Tanks: Status Report. FY 2000 EMSP National Workshop, November 1999, Atlanta, Georgia.

Ward, A.L., G.W. Gee, J.S. Selker, and C. Cooper. 2000. Rapid Migration of Radionuclides Leaked from High-Level Water Tanks: Status Report. FY 2001 EMSP National Workshop, November 2001, Richland, Washington.

Weisbrod, N., T. McGinnis, M. Niemet, and J.S. Selker, 2000. Infiltration Mechanisms of Highly Saline Solutions and Possible Implications for the Hanford Site, EOS Trans. AGU, 81 (48), Fall Meet. Suppl.

Weisbrod, N., J.S. Selker, M.R. Niemet, T. McGinnis, C. Cooper, and A. Ward. 2000. Transport Mechanisms of Highly Concentrated Solutions in Layered Unsaturated Sedimentary Basin, GSA Annual meeting, Reno, NV.

White, M.D, and A.L Ward. 2001. "*Numerical Investigations of Vadose Zone Transport of Saturated Sodium Thiosulfate Solutions."* AGU Fall Meetings, San Francisco, CA, December 5-9, 2001.

Selker, J.S, A.L. Ward, M.R. Niemet, N. Weisbrod, and C. Cooper. 2000. Field Observations of Transport of High Concentration Solutions in Unsaturated Sedimentary Materials. AGU Fall Meeting, San Francisco, California.

9.0 Transitions

The results of this work not yet published are being prepared for publication. Numerical techniques and models resulting from this work are available for public use. The STOMP simulator is already being used for investigating the migration of high salinity fluids at Hanford. The code is available for download at http://www.pnl.gov/etd/stomp.

10.0 Patents

No patents were filed during the course of this work.

11.0 Future Work

The overall goals of this project was to identify the conditions under which fingering might occur during the infiltration of hypersaline fluids and to determine whether fingering was an important mechanism of transport in Hanford's waste management areas. Not only were these goals exceeded, but this work has led to the identification of issues that require further study. These studies have shown that elevated density, viscosity and surface tension interact to impact the behavior of hypersaline fluids in the subsurface under controlled temperatures. Although all of our studies were conducted under isothermal conditions, it is well known that tank wastes at Hanford were often quite hot. Therefore, an important extension of this study will be to investigate the temperature effects on wetting contact angle and the capillary pressure-saturation curves, particularly the liquid entry pressure of the wetting curve. While these phenomena will not limit the use of our findings in predicting the future migration of contaminants, a better understanding of these phenomena will be required for history matching of existing plumes.

It was also shown that due to the high-sodium content of the tank wastes the colloids were deflocculated below a critical salt concentration in Hanford sediments. The released colloids, which at the site would be expected to carry the bulk of the sorbed heavy metals and radioisotopes, were mobile though coarse Hanford sediments, but clogged finer layers. These colloidal processes greatly complicate the prediction of vadose movement of radionuclides and will require considerable additional investigation. Field observations show that flow is dominated by micro-scale layering and strong anisotropy. Leaked materials may therefore flow preferentially along the fine layers that act as capillary barriers and would be further driven by water vapor delivered from the coarse materials above and below the band of transport. Given the efficiency of such vapor delivery down to concentrations on the order of 0.01 those seen in leaked wastes, this process could lead to much grater lateral spreading than would be expected from a simple analysis of the volume of waste entering the environment and will have very

important ramifications for remediation options in which waste is left in the ground and should be studied further. However, standard practices for predicting transport under unsaturated conditions do not account for the random heterogeneity and strong anisotropy that can be expected under the extremes of nonlinear flow behavior typical of Hanford's vadose zone. Variable anisotropy, an extreme of nonlinear behavior, can both subdue and enhance predicted migration rates depending on local stratigraphy; enhance nonequilibrium flow; limit access to reactive surfaces; and lead to the costly over-engineering of remediation and risk-management strategies and should receive serious attention.

12.0 Literature Cited

Bergendahl, J. & D. Grasso, 1998. "Colloid Generation During Batch Leaching Tests: Mechanics of Disaggregation." *Colloid Surface A,* 135: 193-205.

Blume, T., N. Weisbrod, and J.S. Selker. 2002. Determination of Critical Salt Concentrations For Particle Release in Homogeneous Silica Sand and Heterogeneous Hanford Sediments. (*In Review*)

Blume, T. 2001. *Critical Salt Concentrations For Particle Release in Homogeneous Silica Sand and Heterogeneous Hanford Sediments*. MS Thesis, Oregon State University

Brooks, R.H. and A.T. Corey. 1964. *Hydraulic properties of Porous Media*. Colorado State University, Hydrology Paper No. 3, 27 pp.

United States Department of Energy-Grand Junction Projects Office (DOE-GJPO). 1998. *Vadose Zone Characterization Project at the Hanford Tank Farms: BX Tank Farm Report,* GJO-98-40-TAR (GJPO-HAN-19), Grand Junction, Colorado.

Felmy, A. R. 1995. "*GMIN, A computerized chemical equilibrium program using a constrained Minimization of the Gibbs Fee Energy: Summary Report*." pp 377-407, In Chemical Equilibrium and Reaction Models, SSSA Special Publication 42, American Society of Agronomy, Madison, WI.

Guggenheim, E.A., and N.K. Adam. 1933. "The thermodynamics of adsorption at the surface of solutions." *Proc. R. Soc., London*. 139A:218.

Kelly, S.F, and J.S. Selker. 2001. "Osmotically driven water vapor transport in unsaturated soil." *Soil Sci. Soc. Am. J*. 65:1634-1641.

Kung, K-J. S. 1990. "Preferential flow in a sandy vadose zone: 1. Field observation." *Geoderma*, 46:51-58.

Letey, J., J. Osborn, and R. E. Pelishek (1962). "Measurement of Liquid-Solid Contact Angles in Soil and Sand." Soil Science 93: 149-153.

Li, Z-B, Y-G. Li, and J-F. Lu. 1999. "Surface Tension Model for Concentrated Electrolyte Aqueous Solutions by the Pitzer Equation." *Ind. Eng. Chem. Res*. 38: 1133-1139.

Malik, R.S, S. Kumar, and I.S. Dahiya. 1984. "An Approach to Quick Determination of some Water Transmission Characteristics of Porous-Media." *Soil Sci.* 137: 395-400.

McGinnis, T. 2001. "*Determining Contact Angle of Solutions with Varying Surface Tension on Dry and Pre-wetted Silica Sands*." MS Thesis Oregon State University Bioengineering.

McGinnis, T, J.S. Selker, and N. Weisbrod. 2002. "Determining Contact Angle of Solutions with Varying Surface Tension on Dry and Pre-wetted Silica Sands." (*In Review*)

National Academy of Science. 2000. *Research Needs in Subsurface Science*. National Academy Press, Washington, D.C.

Nassar, I.N, and R. Horton. 1989. "Water Transport in Unsaturated Nonisothermal Salty Soil: 1. Experimental Results." *Soil Sci. Am. J.* 43:1323-1329.

Nieber, J.L. 1996. "Modeling finger development and persistence in initially dry porous media." *Geoderma* 70:207-229.

Niemet, M.R., and J.S. Selker. 2001. "A New Method for Quantification of Liquid Saturation in 2D Translucent Porous Media Systems using Light Transmission." *Adv. Water Res.* 24, 651-666.

Niemet, M. R., M.L. Rockhold, N. Weisbrod, and J. S. Selker. 2002. "The Relationship Between Gas-liquid Interfacial Surface Area, Liquid Saturation and Light Transmission." (*In Review*).

Ross, B. 1990. "The Diversion Capacity of Capillary Barriers." *Water Resour. Res*. 26: 2625-2629.

Rouston, R.C., W.H. Price, D.J. Brown, and K.R. Fecht. 1979. "*High Level Waste Leakage from the 241-T-106 Tank at Hanford".* RHO-ST-14. Rockwell Hanford Operations, Richland, Washington.

Rulison, Christopher (1996). "*Wettability Studies for Porous Solids Including Powders and Fibrous Materials*." Charlotte, NC, Kruss USA.

Selker, J. 1997. "Design of Interface Shape for Protective Capillary Barriers." *Water Resour. Res* 33: 259-260.

Selker, J.S., T.S. Steenhuis, Y.-J. Parlange 1992. "Wetting Front Instability in Homogeneous Sandy Soils Under Continuous Infiltration." *Soil Sci. Soc. Am. J.* 56:1346-1350.

Trompert, R.A. 1993. "Local-uniform-grid Refinement and Transport in Heterogeneous Porous Media." *Adv. In Water Resour*. 16: 293-304.

Ward, A.L., and G.W. Gee. 2001. "The Influence of Fluid Interfacial Characteristics on the Wetting of Mineralogically Heterogeneous Porous Media." (*In Review*)

Ward, A.L., G.W. Gee, and C.S. Simmons. 2002. "The Concept of a Dynamic Contact Angle to Describe the Capillary Rise of Hypersaline Fluids." (*In Review*)

Ward, A.L., and G.W. Gee. 2002. "Prediction of Liquid-entry Pressures on the Basis of Fluid Composition." (*In Review*)

Ward, A.L. and M.D. White. 2002. "Continuum-scale Modeling of Hypersaline Fingers in Unsaturated Porous Media With an Adaptive-Grid Method." (*In Preparation*)

Ward, A.L., G.W. Gee, J.S. Selker, and C. Cooper. 1999. "*Rapid Migration of Radionuclides Leaked from High-Level Water Tanks: Status Report*." FY 2000 EMSP National Workshop, November 1999, Atlanta, Georgia.

Ward, A.L., M.D. White, G.W. Gee, N. Weisbrod, J.S. Selker, and C. Cooper. 2000. "Incorporating the Effect of Fluid Constitution on Surface Tension and Equilibrium Contact Angle into Predictions of Hypersaline Fluid Migration in Unsaturated Soils." *EOS Trans. AGU*, 81 (48), Fall Meet. Suppl..

Washburn, E. W. (1921). "The Dynamics of Capillary Flow." *Physical Review* 17: 273.

Weast, R.C. (Ed.), *CRC Handbook of Chemistry and Physics*, 57th ed., CRC Press, Boca Raton, Fla., 1977.

Weisbrod, N., M. Niemet, M. Rockhold, T. McGinnis, and J.S. Selker. 2002a. "Infiltration of Saline Solutions into variably saturated porous media." (*In Review).*

Weisbrod, N., M. R Niemet, T. McGinnis, and J.S. Selker. 2002b. "Vapor Flow in the Vicinity of Saline Plumes: Homogeneous and Layered Unsaturated Porous Media." (*In Review*)

Weisbrod, N., T. McGinnis, M. Niemet, and J.S. Selker, 2000. "Infiltration Mechanisms of Highly Saline Solutions and Possible Implications for the Hanford Site, *EOS Trans. AGU*, 81 (48), Fall Meet. Suppl..

Weisbrod, N., M. Niemet, M. Rockhold, T. McGinnis, and J.S. Selker, 2001. Infiltration of Saline Solutions into variably saturated porous media. (*In Review*).

White, M.D., and M. Oostrom. 2000. *STOMP Subsurface Transport Over Multiple Phases, Version 2.0, Theory Guide,* PNNL-12034, UC-2010, Pacific Northwest National Laboratory, Richland, Washington.

Wraith, J.M., and D. Or, Nonlinear parameter estimation using spreadsheet software, *J. Natural Resour. Life Sci. Ed.*, 27: 13-19.

Young, M.H., Karagunduz, A., Šimůnek, J., and K.D. Pennell. 2002. "A modified upward Infiltration Method for Characterizing Soil Hydraulic Properties, *Soil Sci. Soc. Am. J.*, 66:57-64.

13.0 Feedback

The EMSP Annual meetings are welcomed opportunities for principle investigators to interact, report progress, and develop strategies for moving forward. Investigators have been required to provide electronic copies of posters and presentations for posting on meeting websites. While this provides exposure for the program and publicizes research findings as they develop, it is inconsistent with good science. Research results should be made available to the public in scientific publications after peer review. Publication of work in progress on websites and other documents creates a permanent record that includes incomplete or subsequently unimportant finds. A good example is in our work where the results of our early efforts to model density-driven fingering were presented at the Atlanta workshop and "published" were subsequently

found to be limited by an inappropriate conceptualization. Publication of work in progress should e limited to title summaries or abstracts and should not include the full presentation or posters.